



Spatial patterns of biphasic ectoenzymatic kinetics related to biogeochemical properties in the Mediterranean Sea.

France Van Wambeke¹, Elvira Pulido¹, Julie Dinasquet^{2,3}, Kahina Djaoudi^{1,4}, Anja Engel⁵, Marc Garel¹, Sophie Guasco¹, Sandra Nunige¹, Vincent Taillandier⁶, Birthe Zäncker^{6,7}, Christian
5 Tamburini¹.

¹Aix-Marseille Université, CNRS/INSU, Université de Toulon, IRD, Mediterranean Institute of Oceanography (MIO) UM 110, 13288, Marseille, France

²Marine Biology Research Division, Scripps Institution of Oceanography, UCSD, La Jolla, USA

10 ³Sorbonne Universités, UPMC University Paris 6, Laboratoire d'Océanographie Microbienne (LOMIC), Observatoire Océanologique, 66650, Banyuls/mer

⁴Molecular and Cellular Biology, The University of Arizona, Tucson, USA

⁵GEOMAR – Helmholtz-Centre for Ocean Research, Kiel, Germany

15 ⁶CNRS, Sorbonne Universités, Laboratoire d'Océanographie de Villefranche (LOV), UMR7093, 06230 Villefranche-sur-Mer, France

⁷The Marine Biological Association of the UK, Plymouth, United Kingdom

Correspondence to: F. Van Wambeke (france.van-wambeke@mio.osupytheas.fr)

Abstract. Prokaryotic ectoenzymatic activity, abundance and heterotrophic production were
20 determined in the Mediterranean Sea, within the epipelagic and the upper part of the mesopelagic layers. The Michaelis-Menten kinetics were assessed, using a range of low (0.025 to 1 μM) and high (0.025 to 50 μM) concentrations of fluorogenic substrates. Thus, K_m and V_m parameters were determined for both low and high affinity systems for alkaline phosphatase (AP), aminopeptidase (LAP) and β -glucosidase (βGLU). Based on the constant derived from the high AP affinity system,
25 *in-situ* hydrolysis rates of N-protein contributed of $48\% \pm 30\%$ for the heterotrophic prokaryotic nitrogen demand within epipelagic waters and of $180\% \pm 154\%$ within deeper layers. LAP hydrolysis rate was higher than bacterial N demand only within the deeper layer, and only based on the high affinity system. Although ectoenzymatic hydrolysis contribution to heterotrophic prokaryotic need was high in terms of N, but low in terms of C. Based on a 10% bacterial growth
30 efficiency, the cumulative hydrolysis rates of C-proteins and C-polysaccharides contributed to a small part of the heterotrophic prokaryotic carbon demand, on average $2.5\% \pm 1.3\%$ in the epipelagic layers. This study notably points out the biases in current and past interpretation of the relative activities differences among the 3 tested enzymes, in regard to the choice of added concentrations of fluorogenic substrates. In particular, enzymatic ratios LAP/ βGLU , as well as
35 some trends with depth, were different considering activities resulting from the high or the low affinity system.

1. Introduction

Most of the organic matter being in the state of high molecular weight material, its hydrolysis by ectoenzymes plays an important role in the degradation, utilization and mineralization processes in
40 aquatic environments, but also in nutrient's regeneration (Hoppe, 1983; Chróst, 1991). Whether or not the ectoenzymatic activity must be considered as a limiting rate in organic matter remineralization is subject of debate as hydrolysis and consumption of hydrolysis products are not always coupled (e.g. for instance Smith et al., 1992). Bacterial ectoenzymatic hydrolysis is usually determined using fluorogenic substrates (Hoppe, 1983) which, upon cleavage by ectoenzymes,
45 trigger the release of a fluorescent by-product. The increase of the latter is monitored by fluorimetry over time, allowing quantification of ectoenzymatic hydrolysis rates. Kinetic experiments are time-



consuming and most studies reporting ectoenzymatic activity seldomly examine enzyme kinetic patterns, but only assess activity based on one substrate concentration assumed to be saturating. Baltar et al. (2009b) report that among 17 published studies, 12 used a single range of substrate concentrations, varying from 0.02 to 1000 μM (with a median of 50 μM), and only 5 considered variable ranges. Within these 5 studies, for the concentration kinetic, the minimum concentration used was 50 nM at the lowest, and was more generally between 1 and 5 μM , and the highest concentration used ranged between 5 μM and 1200 μM , median 200 μM . In the Mediterranean Sea, a compilation of data by Zaccone and Caruso (2019) shows that among 22 studies, 6 used a single concentration (that they assumed to be saturating) with a median of 125 μM for MCA-leu and 50 μM for MUF-P. While the other studies assessed kinetics systematically, the range of concentrations was again highly variable (min 0.025 - 200 median 0.1 μM , max 1 - 4000 median 20 μM). However, the combination of: i) non-specific target of the enzymes, ii) the heterogeneity of enzymatic systems among a single species, iii) the diversity of present species and iv) the concentration of surrounding substrates, will result in multiphasic kinetics (Chróst, 1991; Arnosti, 2011; Sinsabaugh and Shah, 2012 and ref therein). It is well known that ectoenzymes can be produced by a diversity of microorganisms. Their activity depends on a patchy distribution of natural substrates, and a variety of natural (potentially unknown) molecules hydrolyzed by the same enzymes that hydrolyze the added fluorochrome, all probably having different affinities for the enzyme. Indeed, cell-specific activities and types of activities were shown to be extremely variable among 44 isolated strains, cultivated in batch cultures and sampled during exponential phase (Martinez et al., 1996). Arrieta and Herndl (2001) assessed the diversity of marine bacterial β -glucosidases from a natural community separated using capillary electrophoresis zymography and showed that they had different K_m and V_m . Biphasic kinetic systems have been described in areas where increasing gradients of polymeric material are expected due to the high concentration of particles; e.g. near bottom water and sediment for aminopeptidase (Tholosan et al., 1999), in a shallow bay for phosphatases (Bogé et al., 2013). Moreover, in the water column different kinetic systems were also observed and are generally attributed to attached or free-living bacteria having different affinities for substrates, k-strategists-oligotrophic bacteria (with low K_m and low V_m) or r-strategists/copiotroph bacteria (with high K_m and V_m , Koch, 2001). At depth, the simultaneous presence of more refractory DOM with recent and freshly sedimenting particles, suggests also possible multiphase kinetics for ectoenzymatic activity. Varying kinetic parameters were also attributed to 'free' (i.e. related to free-living bacteria) *versus* 'attached' heterotrophic bacteria, the latter highlighting higher both V_{max} and K_m , i.e. adapted to cope with high substrate concentrations (Unanue et al., 1998). Due to the soluble nature of the fluorochrome released, these estimates are based on size fractionation prior the incubations, which biases ectoenzymatic activities in each size fraction, due to filtration artifacts and disruption of trophic relationships between primary producers, heterotrophic bacteria, regenerative protozoans and osmotrophs. Nevertheless, most studies have shown that cell-specific ectoenzymatic activities on aggregates are ~10 fold higher than those of the surrounding assemblages (decaying bloom, Martinez et al., 1996). Furthermore, carbon budgets have shown that the prokaryotes attached to aggregates are likely a source of by-products for free-living prokaryotes, thanks to their ectoenzymatic hydrolysis (Smith et al., 1992). The use of bulk water concentration kinetics allows the determination of different enzymatic kinetics without disturbing relationships between free/attached prokaryotes and DOM/POM interactions during the incubations.

In the Mediterranean Sea, elemental C/N/P ratios of nutrients and organic matter are the object of particular attention and debates, especially when it comes to the origin of P-deficiency and DOC



accumulation (Thingstad and Rassoulzadegan, 1995; Krom et al., 2004). The export of organic carbon in dissolved vs. particular forms is related to the P-limitation status within surface layers
95 (Guyennon et al., 2015). Therefore, models used to compute C, N and P budgets in the Mediterranean Sea must consider non-Redfield C/N/P stoichiometry (Baklouti et al., 2006). The interaction between different enzymes has been largely studied in the Mediterranean Sea (Zaccone and Caruso, 2019) due to the particular role of this elemental stoichiometry. Indeed, the epipelagic layers are P or N-P limited during most periods of water mass stratification, and ectoenzymes
100 providing P and N sources from organic matter, such as aminopeptidase and phosphatase have been intensively studied as indicators of these limitations (Sala et al., 2001; Van Wambeke et al., 2002). However, the potential bias introduced by multiple kinetics, when comparing different types of ectoenzymes, is still poorly understood.

In this study, we investigated in the Mediterranean Sea, the kinetics of three series of enzymes targeting
105 proteins, phospho-mono esters and carbohydrates (aminopeptidase, alkaline phosphatase and β -D – glucosidase, respectively) in relation to the elemental stoichiometry of particulate and dissolved organic matter. We have paid particular attention to the use of a wide range of substrates concentrations to evaluate potential multiphasic kinetics. Our aim was to study the effects of the respective activities of the ectoenzymes in relation to the quality of the available organic matter, below the productive layer
110 and above the deep Mediterranean waters. We were especially interested in the Levantine Intermediate Waters (LIW), a typical Mediterranean water mass that spreads from ~200 to 700 m, characterized by a local maximum of salinity and a local minimum of dissolved oxygen concentration (e.g. Kress et al., 2003; Malanotte-Rizzoli et al., 2003). This study focuses on the open waters of the western Mediterranean Sea and Ionian Sea, considering four water layers: surface (generally P or N limited
115 during the stratification period), the deep chlorophyll maximum layer (coinciding with nutricline depths), the LIW and below the LIW. Finally, we discuss the biases in interpretation of past and current enzymatic kinetic, potentially induced by the reduced range of used substrate concentrations. The data used in this ms are also developed in another article (Van Wambeke et al, in prep) of the special issue in which all biogeochemical fluxes (phytoplankton and heterotrophic bacterial P and N demand, N₂
120 fixation rates, aminopeptidase, phosphatase activities) within the mixed layers will be compared with wet and dry N and P atmospheric fluxes thanks to an exceptional simultaneous measurements of all these fluxes during the same cruise.

2. Materials and Methods

2.1 Sampling strategy

125 The PEACETIME cruise (doi.org/10.17600/15000900) was conducted in the Mediterranean Sea, from May to June 2017, along a transect extending from the Western Basin to the center of the Ionian Sea (25°S 115 E – 15°S, 149°W, Fig. 1). For details on the cruise strategy, see Guieu et al. (2020). Stations of short duration (< 8 h, 15 stations named SD1 to SD10, Fig. 1) and long duration (5 days, 3 stations named TYR, ION and FAST) were sampled. Generally, at least 3 casts were
130 conducted at each short station. One focused on the epipelagic layer (0 - 250 m), and the second one focused on the whole water column. Both were sampled with a standard, classical-CTD rosette equipped with a sampling system of 24 Niskin bottles (12 L), and a Sea-Bird SBE9 underwater unit equipped with pressure, temperature (SBE3), conductivity (SBE4), fluorescence (Chelsea Acquatracka) and oxygen (SBE43) sensors. The third cast, from surface to bottom was performed
135 under ‘trace metal clean conditions’ using a second instrumental package (called TMC-rosette) mounted on a Kevlar cable and equipped with Go-Flo bottles that were sampled in a dedicated trace



metal free-container. The long stations were abbreviated as TYR (situated in the center of the Tyrrhenian Basin), ION (in the center of the Ionian Basin), FAST (in the western Algerian Basin). Long stations were selected using satellite imagery, altimetry and Lagrangian diagnostics and expected events of rain (Guieu et al., 2020). At these stations, repeated casts were performed during at least 5 days, alternating CTD- and TMC- rosettes.

The water sampled with the conventional CTD-rosette, was used for measuring heterotrophic prokaryotic production (BP), heterotrophic prokaryotic abundances (BA), ectoenzymatic activity (EEA), chlorophyll stocks, particulate organic carbon (POC), nitrogen (PON) and phosphorus (POP) and dissolved organic carbon (DOC). The TMC-rosette was used for dissolved inorganic nitrogen (DIN) and phosphorus (DIP), dissolved organic nitrogen (DON) and phosphorus (DOP).

Besides measurements of the biogeochemical variables, BP and ectoenzymatic activities described below, other data presented in this paper include hydrographic properties (T, S, O₂), total chlorophyll a (Tchl_a) concentrations for which detailed protocols of analysis and considerations for methodology are available in Taillandier et al. (2020), Guieu et al. (2020), and Maranon et al. (2020)

We focused on 4 layers of the water column: two were in the epipelagic waters: surface (5 m, named 'surf'), and the deep chlorophyll maximum layer, localized by the *in vivo* fluorescence continuously measured by the instrumental package during downcasts (named 'dcm'); and two deeper layers: one in the LIW (localized by maximum salinity and minimum oxygen properties during downcasts, named 'liw'), and second sampled at 1000 m (the limit between meso and bathypelagic waters), except at 2 stations (FAST, 2500 m; ION, 3000 m) named 'mdw'. Table 1 resumes the sampled stations with their localization, characteristics and depths of 'dcm', 'liw' and 'mdw' layers sampled.

2.2 Biochemistry

Nitrate (NO₃), nitrite (NO₂), and orthophosphate (DIP) concentrations were determined on a segmented flow auto-analyzer (AAIII HR Seal Analytical) according to Aminot and K erouel (2007). The quantification limits were 0.05 μM for NO₃, 0.01 μM for NO₂ and 0.02 μM for DIP. The dissolved organic pools, DON and DOP, were determined after high-temperature (120 $^{\circ}\text{C}$) persulfate wet oxidation mineralization (Raimbault et al., 1999). Twenty ml of water sample were filtered on a 0.2 μm PES membrane and collected into 25 ml glass flasks. Samples were immediately poisoned with 100 μl H₂SO₄ 5N and stored in the dark until analysis in the laboratory. For DON and DOP, filtered samples were then collected in Teflon vials adjusted at 20 ml for wet oxidation. Nitrate and phosphate formed after the wet persulfate oxidation, corresponding to total dissolved pool (TDN and TDP), were then determined as previously described for the dissolved inorganic pools. DON and DOP were obtained by the difference between TDN and DIN, and TDP and DIP, respectively. The limits of quantification were 0.5 and 0.02 μM for DON and DOP, respectively.

The particulate pools (PON, POP) were determined using the same wet oxidation method (Raimbault et al., 1999). A volume of 1.2 L was collected from Niskin bottles in polycarbonate bottles and directly filtered through a pre-combusted (450 $^{\circ}\text{C}$, 4 h) glass fiber filter (Whatman 47mm GF/F) and kept frozen at -20 $^{\circ}\text{C}$ until return to the laboratory. For the analysis, filters were placed in Teflon vials with 20 mL of ultrapure water (Milli-Q grade) and 2.5 mL of the wet oxidation reagent for mineralization. Nitrate and orthophosphate produced were analyzed as



180 described previously. The limits of quantification were 0.02 and 0.001 μM for PON and POP,
respectively.

Within epipelagic, nutrient depleted layers DIP and NO_3 were also determined using the LWCC
method (Zhang and Chi, 2002) in which the sensitivity of the spectrophotometric measurement is
improved by increasing the optical path length of the measurement cell to 2.5 m. For DIP,
185 quantification limits were decreased down to 0.8 nM and the response is linear up to about 150 nM,
for NO_3 , quantification limits decreased to 9 nM.

Samples for dissolved organic carbon (DOC) were filtered through two pre-combusted (24 h,
450°C) glass fiber filters (Whatman GF/F, 25 mm) using a custom-made all-glass/Teflon filtration
syringe system. Samples were collected into pre-combusted glass ampoules and acidified to pH 2
190 with phosphoric acid (H_3PO_4). Ampoules were immediately sealed until analyses by high
temperature catalytic oxidation (HTCO) on a Shimadzu TOC-L analyzer (Cauwet, 1999). Typical
analytical precision is ± 0.1 -0.5 (SD) or 0.2-0.5% (CV). Consensus reference materials
(<http://www.rsmas.miami.edu/groups/biogeochem/CRM.html>) was injected every 12 to 17 samples
to insure stable operating conditions. Particulate organic carbon (POC) was measured using a CHN
195 analyzer and the improved analysis proposed by Sharp (1974).

Samples (20 ml) for total hydrolysable carbohydrates (TCHO) > 1 kDa were filled into
precombusted glass vials (8 h, 500°C) and stored at -20°C until analysis. Samples were desalinated
with membrane dialysis (1 kDa MWCO, Spectra Por) at 1°C for 5 h. Samples were hydrolyzed for
20 h at 100°C with 0.8 M HCl final concentration with subsequent neutralization using acid
200 evaporation (N_2 , for 5 h at 50°C). TCHO were analysed using high performance anion exchange
chromatography with pulsed amperometric detection (HPAEC-PAD) which was applied on a
Dionex ICS 3000 ion chromatography system (Engel and Händel, 2011). Two replicates per TCHO
sample were analyzed.

Total hydrolysable amino acids (TAA) were determined from 5 mL of sample which was filled into
205 precombusted glass vials (8 h, 500°C) and stored at -20°C. Samples were measured in duplicates.
The samples were hydrolyzed at 100°C for 20 h with 1 mL 30% HCl (Suprapur[®], Merck) to 1 ml of
sample added and neutralized by acid evaporation under vacuum at 60°C in a microwave.
Remaining acid was removed with water. Samples were analyzed by high performance liquid
chromatography (HPLC) using an Agilent 1260 HPLC system following a modified version of
210 established methods (Lindroth and Mopper, 1979; Dittmar et al., 2009). Prior to the separation of 13
amino acids with a C^{18} column (Phenomenex Kinetex, 2.6 μm , 150 x 4.6 mm), in-line derivatization
with o-phthalaldehyde and mercaptoethanol was performed. A gradient with solvent A containing
5% acetonitrile (LiChrosolv, Merck, HPLC gradient grade) in sodium dihydrogen phosphate
(Suprapur[®], Merck) buffer (pH 7.0) and solvent B being acetonitrile was used for analysis. A
215 gradient from 100% solvent A to 78% solvent A was produced in 50 min.

2.3 Bacterial production

Bacterial production (BP, *sensus stricto* referring to prokaryotic heterotrophic production) was
determined onboard using the microcentrifuge method with the ^3H - leucine (^3H -Leu) incorporation
technique (Smith and Azam, 1992) within epipelagic waters, and the filtration technique for deep
220 waters, as the centrifuge technique is limited to incubation volumes of 1.5 mL and was not
sufficiently sensitive in deep waters. In epipelagic waters, triplicate of 1.5 mL samples and a killed
control with trichloroacetic acid (TCA, 5% final concentration) were incubated with a mixture of



[4,5-³H]-leucine (Amersham, specific activity 112 Ci mmol⁻¹) and non-radioactive leucine at final concentrations of 7 and 13 nM, respectively. Samples were incubated in the dark at the respective *in situ* temperatures for 1- 4 h. On 9 occasions, we checked that the incorporation of leucine was linear with time. Incubations were ended by the addition of TCA to a final concentration of 5%, followed by three runs of centrifugation at 16000 g for 10 minutes. Bovine serum albumin (BSA, Sigma, 100 mg L⁻¹ final concentration) was added before the first centrifugation. After discarding the supernatant, 1.5 mL of 5% TCA was added before the second centrifugation, and for the last run, after discarding the supernatant, 1.5 mL of 80% ethanol was added. The ethanol supernatant was discarded and 1.5 mL of liquid scintillation cocktail (Packard Ultimagold MV) was added. For 'liw' and 'mdw' layers, 40 mL samples were incubated in the dark for up to 12 hours at the *in situ* temperature (triplicate live samples and one formalin-fixed control), fixed with formalin (2% final concentration), using 10 nM [4,5-³H]-leucine. After filtration of the sample through 0.2 μm polycarbonate filters, 5% TCA were added for 10 minutes, and then the filter was rinsed with an additional 10 mL rinse with 5% TCA and a final 80% ethanol rinse.

For both types of samples (centrifuge tubes and filters) the radioactivity incorporated into macromolecules was counted in a Packard LS 1600 Liquid Scintillation Counter on board the ship. A factor of 1.5 kg C mol leucine⁻¹ was used to convert the incorporation of leucine to carbon equivalents, assuming no isotopic dilution (Kirchman, 1993), as checked from occasional concentration kinetics. Standard deviations associated with the variability between triplicate measurements averaged 8% and 25% for BP values estimated with the centrifugation (higher activities surface layers) or the filtration technique (lower activities, deep layers), respectively.

2.4 Ectoenzymatic activities

Ectoenzymatic activities were measured fluorometrically, using fluorogenic model substrates that were L-leucine-7-amido-4-methyl-coumarin (Leu-MCA), 4 methylumbelliferyl – phosphate (MUF-P), 4 methylumbelliferyl – βD-glucopyranoside (MUF-βglu) to track aminopeptidase activity (LAP), alkaline phosphatase activity (AP), and β–glucosidase activity (βGLU), respectively (Hoppe, 1983). Stocks solutions (5 mM) were prepared in methycellosolve and stored at –20°C. Release of the products of LAP, AP and βGLU activities, MCA and MUF, were followed by measuring increase of fluorescence (exc/em 380/440 nm for MCA and 365/450 nm for MUF, wavelength width 5 nm) in a VARIOSCAN LUX microplate reader. The instrument was calibrated with standards of MCA and MUF solutions diluted in < 0.2 μm filtered and boiled seawater. For measurements, 2 mL of unfiltered seawater samples were supplemented with 100 μL of a fluorogenic substrate solution diluted so that different concentrations were dispatched in a black 24-well polystyrene plate in duplicate (0.025 to 50 μM). Three plates were filled per layer analyzed with the different substrates MUF-P, MCA-leu and MUF-βglu. Incubations were carried out in the dark in thermostatically controlled incubators reproducing *in situ* temperature ranges. Incubations lasted up to 24 h long with a reading of fluorescence every 1 to 3 h, depending on the intended activities. The rate was calculated from the linear part of the fluorescence *versus* time relationship. Boiled-water blanks were run to check for abiotic activity. From varying velocities obtained, we determined the parameters V_{max} (maximum hydrolysis velocity) and K_m (Michaelis-Menten constant which reflects enzyme affinity for the substrate) by fitting the data using a non-linear regression on the following equation: $V = V_{max} \times S / (K_m + S)$, where V is the hydrolysis rate and S the fluorogenic substrate concentration added. We determined V_m and K_m using 2 series of substrate concentrations: V_{m50} and K_{m50} were calculated using a range of 11 concentrations



(0.025, 0.05, 0.1, 0.25, 0.5, 1, 2.5, 5, 10, 25 and 50 μM) in duplicate and V_{m1} and K_{m1} were calculated using a restricted range of substrate concentrations up to 1 μM (0.025, 0.05, 0.1, 0.25, 0.5, 1 μM) in duplicate. We used the term ‘ectoenzyme’ and considered that it included all types of enzymes found outside the cell, including enzymes fixed on cells (on external membranes, or within the periplasmic space), and free-dissolved enzymes, to broadly encompass all enzymes located outside intact cells regardless of the process by which such enzymes entered the environment.

We used an approach similar to Hoppe et al. (1993) to compute *in situ* hydrolysis rates for LAP and βGLU (we did not make this calculation for AP as this is developed in a companion paper from this special issue in Pulido-Villena et al., in prep). We used total carbohydrates (TCHO) and total aminoacids (TAA) data and assuming they could be representative of dissolved combined carbohydrates and dissolved proteins, respectively. *In situ* hydrolysis rates of LAP and βGLU were determined using molar concentrations of TAA and TCHO used as substrate concentration in the Michaelis-Menten kinetics, respectively. These rates were calculated based on V_{m1} K_{m1} , in one hand and on V_{m50} and K_{m50} , on the other hand. The transformation of *in situ* hydrolysis rates expressed in $\text{nmol L}^{-1} \text{h}^{-1}$ were then transformed in carbon units using C per mole TCHO, C per mole TAA, and in nitrogen units using N per mole TAA, as the molar distributions of TAA and TCHO were available.

2.5 Statistics

Trends with depth were estimated using a depth variation factor (DVF) calculated as the mean of pooled ‘surf’ and ‘dcm’ data divided by the mean of pooled ‘liw’ and ‘mdw’ data. This decrease (or increase), was considered as significant after a t-test comparing both series of data. The type of t test used depended on the result of a preliminary F-test checking for variance. The prism 4 (Graph Pad software, San Diego, USA) was used to perform nonlinear regressions on Michaelis-Menten kinetics. Means are cited \pm standard errors. Correlations between variables were examined after log transformation of the data.

3. Results

3.1 Hydrological situations.

The sampled stations have basins and latitude characteristics that were superimposed on a changing the seasonal pattern. Lower surface temperatures (14 - 17°C) were thus measured at ST1 to ST3, sampled in the beginning of the cruise at higher latitudes, and higher temperatures at ST10 (21.6°C) were sampled at the end of the cruise. T/S diagrams presented profiles characteristic of the different basins and water masses (Fig. 2). Modified Atlantic Waters (MAW) are characterized by low salinity below the seasonal thermocline; this property is stretched in the westernmost stations, then progressively relaxes on eastern station, revealing an eastward circulation in the Algerian Basin and a dispersion in the connected basins (northwestern Mediterranean, Tyrrhenian, and Ionian Seas). Levantine intermediate waters (LIW) lying at depths of 200 to 700 m are characterized by local salinity maximum in the T/S diagram. This property is pronounced in the eastern stations and progressively lowered on the western stations, revealing an opposite circulation pattern to the MAW. The western and eastern Mediterranean Deep waters (WMDW and EMDW, respectively) are formed respectively in the northwestern Mediterranean and in the Adriatic-Aegean Seas; they occupy depth ranges below the LIW and are clearly separated by the bathymetric shallow sill at the Sicily strait. The WMDW T/S characteristics (potential temperature 12.91°C, salinity 38.48) were less salty and colder than in the EMDW water mass observed in the Ionian Sea (potential



310 temperature 13.43°C, salinity 38.73). The core of LIW is characterized by lower oxygen content
than its surrounding water masses, shallower (MAW) and deeper (WMDW and EMDW). The core
of LIW becomes colder, less salty and deepened along its main trajectory toward the West. We thus
presented all the figures/tables in the order ST10, FAST, ST1, ST2, ST3, ST4, ST5, TYR, ST6 and
ION, according to the expected circulation of the LIW (from the right to the left). The ‘liw’ samples
315 were situated in a range of 100 m above - 150 m below the core of LIW but were still in its water
mass at all stations. The deeper layer sampled ‘mdw’ corresponded to the top of WMDW water
mass in the Western Basin, was inside the modified WMDW in the Tyrrhenian Basin, and was
inside the EMDW in the Ionian Basin. Note however that ST10 is within an anticyclonic eddy, and
ST3 is influenced by the water dynamics along the continental slope of Sardinia.

320 3.2 Biogeochemical situation

Nitrate and phosphate were depleted in the surface layers, exhibiting concentrations below the
detection limits of the classical methods (0.01 μM , table S1). Using the LWCC technique, however,
DIP was detectable (Table S1) and ranged between 4 to 17 nM at 5 m depth. The depth of nitracline
(roughly estimated from the depth where NO_3 reaches 50 nM) ranged from 30 to 85 m (Table 1).
325 Phosphaclines were deeper in the Eastern basin, with greater differences between the depths of
phosphacline and nitracline, particularly at ST 6 and ION. Chlorophyll content ranged from 18.7 to
35 mg *Tchl a* m^{-2} at ST 6 and ST1, respectively (Table 1). The depth of the deep chlorophyll
maximum ranged from 49 to 83 m in the Western basin, with no particular trend in the Tyrrhenian
Sea and its deepest location was in the Ionian Sea (105 m at ION).

330 The highest DOC values were generally observed within surface layers, and decreased by
approximately 10 μM between layers, the depth variation factor (DVF) ranged from x1.2 to x1.6.
For DON, the DVF was close to that of DOC, ranging from x1.2 to x1.8. Including the 4 layers,
means of DOC/DON and DOC/DOP molar ratios were 14 ± 2 and 2112 ± 1644 , respectively with
no significant trend with depth due to the variability within stations. Means of TAA were stable
335 between ‘surf’ and ‘dcm’ layers, around 210 nM, as the maximum values were either observed
within the surface, or within the ‘dcm’ layers (Table S1, Fig. S1a). At all stations TAA rapidly
decreased between the epipelagic and deeper waters ($p < 0.001$). The mean DVF of TAA (x3.4) was
twice higher than that of DON (x1.5) and this trend was confirmed by contribution of TAA-N to
DON which ranged from between 3 and 9% within the ‘surf’ and the ‘dcm’ layers to between 1.6
340 and 4.6% at the ‘liw’ and ‘mdw’ layers (Fig. S1a) and this contribution decreased significantly with
depth ($p < 0.001$). TCHO ranged from 111 to 950 nM. The contribution of TCHO-C to DOC ranged
from 1.3 to 9.7% according stations and depths. If epipelagic TCHO values were relatively constant
among the different stations (means 595 ± 43 nM in ‘surf’, 351 ± 73 nM in ‘dcm’, Table S1) the
deeper TCHO distributions varied between station as noted for ‘mdw’ layer in ST5, TYR and ST6
345 in the Tyrrhenian Sea where the highest values were obtained (Fig. S1b). At some other stations,
‘mdw’ layers did not display the highest TCHO values but increased compared to ‘liw’ layers. So
that, at 6 stations out of 10, a minimum TCHO value was obtained within ‘liw’ layer (Fig. S1b).
TCHO-C to TAA-C ratio were 4.3 ± 1 , 2.5 ± 0.3 , 5.5 ± 3.5 and 15 ± 14 within ‘surf’, ‘dcm’, ‘liw’
and ‘mdw’ layers, respectively, increasing significantly with depth ($p < 0.02$) and exhibiting
350 particularly high ratios within the Tyrrhenian sea ‘mdw’ layer (ST5 48 TYR 24 , ST6 27).

3.3 Ectoenzymatic activities – kinetic trends

The ectoenzymatic activities were determined using large trophic conditions and over a wide range
of substrate concentrations ranging from 0.025 to 50 μM . Different types of kinetics were obtained



(see examples in Fig. 3). In general, the LAP increased continuously with the concentrations of
355 MCA-leu, the AP stabilized around 1 μM MUF-P, whereas the βGLU showed intermediary
situations. The lowest activities were determined for βGLU (Table 2) and for this enzyme,
measurements were unfortunately below detection limits for most 'liw' and 'mdw' layers.
Occasionally, only few time series showed linear increases of fluorescence with time, coinciding
with the higher range of used concentrations. Consequently, fitting the Michaelis-Menten kinetic
360 was unfortunately impossible. The means of few βGLU rates measurable at depth were $0.010 \pm$
 $0.006 \text{ nmol L}^{-1} \text{ h}^{-1}$ in the 'liw' layer and $0.008 \pm 0.006 \text{ nmol L}^{-1} \text{ h}^{-1}$ in the 'mdw' layer and could be
considered as a minimal value of V_{m50} .

Figures 4 to 6 show the distribution of V_m and K_m for each station and in each layer sampled for
leucine aminopeptidase (LAP), β -glucosidase (βGLU) and alkaline phosphatase (AP). Activities
365 exhibited a large longitudinal variability, particularly AP, even at depth (CV ranged from 101 to
163% according layers, Fig. 4). The lowest longitudinal variability was obtained for βGLU within
surface layers (34% for V_{m50} , 45% for V_{m1}).

In all layers, the highest mean V_m of the 10 stations were obtained for AP, followed by LAP and
then βGLU , whatever the range of tested concentrations (V_{m50} or V_{m1} , Table 2). Within 'surf' AP
370 V_{m50} and AP V_{m1} means were 4 and 6 times higher than their corresponding LAP means,
respectively. Within 'dcm' layers, these values were 6 and 10 times higher, respectively. V_{m50} AP
average was 7 times higher than its corresponding βGLU average within 'surf' (and 5 times at
'dcm') and this factor increased considering V_{m1} (16 and 20 times, respectively at 'surf' and 'dcm'
layers). For each enzyme, the order of magnitude reached for V_{max} was the same at the 'surf' and
375 'dcm' layers.

For LAP (Fig. 4), V_{m50} was on average 3 times higher than V_{m1} in 'surf' and 'dcm' layers, but the
differences between these two rates increased with depth (x9 in 'liw', x12 in 'mdw'). V_{m50}
decreased from epipelagic to mesopelagic waters by a factor of 8 on average, (ratio 'depth variation
factor' – DVF), but by a factor x19 for V_{m1} (Fig. 4a). However, if this decrease was particularly
380 obvious both for V_{m1} and V_{m50} for stations ST10 to ST5 in the Western Basin, it was not the case
for Tyrrhenian waters (ST5, TYR and ST6) where V_{m1} decreased but not V_{m50} . Within ION, V_{m1}
decreased faster than V_{m50} . K_{m50} of LAP showed inconsistent patterns with depth. Some stations
showed a decrease at 'dcm' compared to 'surf' layers (SD10, SD2, TYR, SD6, ION). K_{m50} within
'liw' layers were on the same order of magnitude than at the surface, sometimes even higher
385 (FAST, ST 3, ST5, ST6, ION) as well as in the 'mdw' layers particularly in Tyrrhenian and Ionian
seas (Fig. 4b). For K_{m1} , the trend was a decrease with depth in the western stations (ST10 to ST3)
whereas from stations 4 to ION the order of magnitude of K_{m1} at all depths were the same, with
sometimes a decrease within 'liw' layers (in Tyrrhenian stations).

For βGLU (Fig. 5), V_{m50} was on average 7 and 5 times higher than V_{m1} in 'surf' and 'dcm'
390 layers, respectively. Their differences in V_m were greater than those observed for LAP or AP (Fig.
5a). K_{m50} was of the same order of magnitude at 'surf' and 'dcm' layers or slightly lower (ST1,
ST2, ST3, ST6), but the opposite trend was observed for K_{m1} , which tended to be equal or higher
within 'dcm' layer (Fig. 5b), in particular in the western stations (ST10, FAST, ST2, ST3).

AP was the enzyme for which V_{m1} and V_{m50} were the closest (Fig. 6a), with saturation rates
395 occurring already around 1 μM of added MUF-P (Fig. 3). V_{max50} to V_{max1} ratios were 1.6, 1.3,
2.4 and 3.0 on average for 'surf', 'dcm', 'liw' and 'mdw' layers, respectively. AP within 'surf' layer



showed a larger range of longitudinal variability than the remaining studied ectoenzymes. For instance, V_{m50} ranged from 0.3 to 8.3 $\text{nmol L}^{-1} \text{h}^{-1}$ for AP, compared to 0.08 - 0.23 $\text{nmol L}^{-1} \text{h}^{-1}$ for βGLU and 0.36 - 2.85 $\text{nmol L}^{-1} \text{h}^{-1}$ for LAP (Table 2). The trend within ‘surf’ was an increase of AP towards the east, from a range of 0.8 - 0.9 $\text{nmol L}^{-1} \text{h}^{-1}$ for V_{m50} at ST10 and FAST and up to 8 $\text{nmol L}^{-1} \text{h}^{-1}$ at ION. Both AP V_{m1} and V_{m50} decreased with depth (Fig. 6a), although sometimes both AP V_{m50} and AP V_{m1} at the ‘dcm’ layer were higher than the surface (ST1, 2, 5 TYR, ION). At all stations V_m in ‘mdw’ were equal or lower than those within ‘liw’ layers. About the decline trend with depths, and in opposition with what was described for LAP, we could not see any difference between the eastern and the western stations. DVF was large, varying from x2.8 to x71 for V_{m50} , with lower decreases with depths at ST10 (x2.8) FAST (x3.2) and ST3 (x2.4), and highest DVF at ST1 (x34), ST2 (x71) and ION (x54). V_{m1} and V_{m50} were almost equal (averages of V_{m50}/V_{m1} ratio for the whole data set was 1.6 ± 0.5), and although for AP K_{m50} was on average 7 times higher than K_{m1} , their differences were the lowest compared to the two other enzymes. Average K_{m50}/K_{m1} ratio for βGLU was 320 and average K_{m1}/K_{m50} ratio for LAP was 118. K_{m1} and K_{m50} increased mostly with depth (Fig. 6b) except at ST10. For the other stations, the trend was that K_{m50} increased more with depth (DVF ranged from x2 to x29, seven stations) than K_{m1} (DVF ranged from x1.9 to x3.8, nine stations).

The turnover time of ectoenzymes was determined as the K_m/V_m ratio, which drives the activity at low concentrations of substrates. The incidence of the tested set of substrate concentration is very important on this parameter, as turnover times are systematically lower for the 25-1000 nM substrate range of concentrations (Table 4). The turnover times were the lowest for AP and the highest for βGLU . We estimated the degree of difference between the two-kinetics using the ‘biphasic indicator’ as developed in Tholosan et al. (1999). This index tracks the difference between the initial slopes (V_m/K_m) of Michaelis-Menten kinetics as $(V_{m1}/K_{m1}) / (V_{m50}/K_{m50})$. The biphasic indicator was particularly marked for βGLU (68 in surface and 29 at the dcm), for LAP it increased from about ~4 in ‘surf’ and ‘dcm’ to 10 within ‘liw’ and 20 within ‘mdw’. For AP it stayed more or less constant at the four layers sampled (range 1.9-3.4).

3.4 Specific activities

Both BP and BA were used to compute specific activities (Table 2, Fig S2). Bulk heterotrophic prokaryotic production (BP) was of the same order of magnitude within ‘surf’ and ‘dcm’ layers and decreased by a factor of 59 ± 23 on average within ‘liw’ and ‘mdw’ layers. Per layer, BA was less variable than ectoenzymatic activity or BP. The mean value at epipelagic layers decreased by a factor of 5 in ‘liw’ and by a factor of 10 in ‘mdw’ layer.

For LAP, specific activities per bacterial cell ranged from 0.1 - 2.1 $\times 10^{-18}$ to 0.7 - 13 $\times 10^{-18}$ mol leu cell⁻¹ h⁻¹, based on V_{m1} and V_{m50} rates, respectively (Fig. 7 a, b; Table 3 for V_{m1}). A significant decrease with depth between epipelagic waters and deep waters was obtained only for cell-specific V_{m1} LAP, but not for cell-specific V_{m50} LAP ($p < 0.001$). For AP, per cell-specific activities ranged from 0.11 to 32 $\times 10^{-18}$ mol P cell⁻¹ h⁻¹ and from 0.14 to 39 $\times 10^{-18}$ mol P cell⁻¹ h⁻¹ based on V_{m1} and V_{m50} rates, respectively, not differing significantly due to the low differences between AP V_{m1} and AP V_{m50} (Fig. 7 a, b). Cell-specific AP exhibited either an increase or a decrease with depth (Fig. 8). The depth variation factor (DVF) ranged from x0.1 to x28 (Table 3). Although the t-test gave no significant differences between epipelagic and deep layers for both specific activities, the medians of V_{m1} AP per cell for ‘liw’ and ‘mdw’ layers were lower than those of ‘surf’ and ‘dcm’ (Fig. 7 c, d). Specific prokaryotic production ranged from 1 to 136 $\times 10^{-18}$ g C bact⁻¹ h⁻¹



(Table 3) and always decreased with depth (DVF ranged $\times 4$ - $\times 23$). If only LAP Vm1 rates are considered, while the specific activities per unit cell decreased with depth, the activity per unit BP increased with depth at all stations (Table 3). APVm1 per unit BP tended less to increase with depth than that per unit cell, although a large range of DVF was obtained in both cases according stations
445 for these parameters (Table 3). For all variables (the three enzymes and BP), the trend of specific activities with depth was highly variable among the different stations (Fig. 9). The highest DVF was obtained for BP per cell or AP per cell. Only cell-specific Vm 50 LAP, cell-specific Vm1 AP and cell-specific Vm50 AP sometimes increased with depth.

3.5 In situ hydrolysis rates

450 The *in situ* hydrolysis rates of TAA by LAP are higher using Vm1 and Km1 constants than using Km50 and Vm50, by ~ 3 times in epipelagic but ~ 7 times in deep waters (Fig. 9). Km50 were much higher than TAA concentrations (30 to 400 fold according layers). This difference was still visible but highly lowered considering Km1, as values between TAA and Km1 differed by factor 2 to 5. Consequently, *in situ* TAA hydrolysis rates by LAP based on Km50 and Vm50 represented few
455 percent of Vm50 (means of 13% at 'dcm' to 0.6% at 'mdw'). However, based on Km1 and Vm1, *in situ* rates were relatively higher but in constant proportion relative to Vm1 (30 to 39% according layers).

The *in situ* hydrolysis rate of TCHO by β GLU are higher using Vm1 and Km1 constants than using Km50 and Vm50, by ~ 2.5 times in epipelagic (Fig. 10). Km50 were higher than TCHO
460 concentrations (Table 2, Table S1), by a mean factor of 18 ± 12 within 'surf' and 24 ± 18 at 'dcm' layers. Consequently, *in situ* β GLU hydrolysis rates based on Km50 and Vm50 were quasi proportional to the turnover rate Vm1/Km1 and represented a mean of 7% of the Vm50 in epipelagic layers. At the opposite, Km1 were much lower than TCHO concentrations (by a factor 31 ± 19 in 'surf', 8 ± 7 at the dcm) and thus most *in situ* rates based on Km1 and Vm1 were close to Vm1
465 (93% in 'surf', 79% at the 'dcm').

4. Discussion

4.1 The use of a broader set of substrate concentrations will change our interpretation of ectoenzyme kinetics

470 The idea that ectoenzyme kinetics are not monophasic is not new nor surprising (Sinsabaugh and Shah, 2012 and references therein). But despite the 'sea of gradients' encountered by marine bacteria (Stocker, 2012), multiphasic kinetic is seldom considered. In this work, we compare the low and high concentration ranges of fluorogenic substrates in order to evaluate the possibility of considering the different kinetic parameters in relation to the *in situ* natural concentrations of the
475 substrates. Unanue et al. (1999), in the coastal, epipelagic Mediterranean Sea in winter, used a set of concentration from 1 nM to 500 μ M, revealing biphasic kinetics with a switch between the two phases around 10 μ M for LAP and 1 - 25 μ M for β GLU. They referred to 'low affinity systems' and 'high affinity systems'. They also observed that the differences between the Vm of the two types of enzymes varied according to the range of substrates analyzed. Bogé et al. (2012) used a MUF-P
480 range from 0.03 to 30 μ M and described biphasic AP kinetics in the Toulon Bay, with a switch between the 2 enzymatic systems around 0.4 μ M. The biphasic factor as defined in Tholosan et al (1999) helps to determine the degree of difference between the two Michaelis-Menten kinetics. In our data set, it was 4.5, 3.7, 11 and 20 for LAP in 'surf', 'dcm', 'liw' and 'mdw' layers,



respectively, showing enhanced differences in mesopelagic compared to epipelagic waters. Thus,
485 the differences between these two LAP enzymatic systems could reach differences in the water
column as much as in sediments (Tholosan et al., 1999), in which large gradients of organic matter
lability take place. However, it was not the case for all enzymes, as the differences were the lowest
for AP (biphasic factor 3.3, 1.9, 2.4 and 1.7 in 'surf', 'dcm', 'liw' and 'mdw' layers, respectively)
and relatively consistent with depth. Finally, the difference between the 2 types of enzymes was
490 greater for β GLU (biphasic factor 68 for 'surf' and 29 for 'dcm' layers).

In this study, the use of MUF-P concentrations ranging between 0.025 and 1 μ M highlighted that
AP rates fit well with the Michalis-Menten Kinetic model, with saturations reached at 1 μ M. This
AP activity, responding to a low concentration range, should belong to free-living bacteria and/or
dissolved enzymes (< 0.2 μ m fraction) with affinities adapted to low concentrations of substrates.
495 These results are in agreement with average DOP concentration measured, ranging between 12 and
122 nM in epipelagic waters (Pulido-Villena et al., this issue in prep) and, when detectable, ~ 40 nM
in deep layers. Using fractionation-filtration procedures, much recent works have shown that more
than 50% of the AP activity could be measured in the < 0.2 μ m size fraction (Baltar, 2018 and
references therein), whereas the dissolved fraction of other enzymes is generally lower. Hoppe and
500 Ulrich (1999) found a contribution of the < 0.2 μ m fraction of 41% for AP, 22% for LAP and only
10% for β GLU. We tried during the PEACETIME cruise few size fractionation experiments on
some occasions in 'surf' and 'dcm' layers (results not shown). Although the size-fraction < 0.6 μ m
was filtered only by gravity and a gentle vacuum was applied for the < 0.2 one, AP in the < 0.2 μ m
fraction exceeded the total in 3 cases out of 12. Setting these cases to 100%, we obtained a mean
505 contribution of $60 \pm 34\%$ ($n = 12$) for this size-fraction. However, contributions were on average 25
 $\pm 16\%$ ($n = 12$) for β GLU and $41 \pm 16\%$ ($n = 12$) for LAP for this same size-fraction (< 0.2 μ m),
confirming these trends in the Mediterranean Sea. At the opposite, the higher differences in LAP
V_m and K_m, in response to the range of tested concentrations, suggest development of activities
facing large gradients of substrate concentrations.

510 The use of a large range of concentrations impacted also the K_m values. Indeed, excluding low
concentrations has consequences on the K_m estimation, because if only a high concentration range
is used, the kinetic contribution of any system with high affinity is hidden. Baltar et al. (2009b),
using a concentration of substrates ranging from 0.6 to 1200 μ M, reported an increase in the LAP
K_m (~400 to 1200 μ M) and AP K_m (~2 to 23 μ M) with depth down to 4500 m in the sub-tropical
515 Atlantic. In contrast, Tamburini et al. (2002), using a concentration of substrates ranging from 0.05
to 50 μ M, obtained lower K_m values (ranging between 0.4 and 1.1 μ M) for LAP in the
Mediterranean deep waters (down to 2000 m depth). It is however difficult to conclude about the
effect of the substrate concentration on K_m variability with depth by comparing 2 studies from
different environments. In our study where both kinetics were determined in the same waters, we
520 came to different conclusions considering K_{m50} or K_{m1}: if LAP K_{m1} is on average x 24 (surf) to x
8 (dcm) higher than β GLU K_{m1}, K_{m50} were in the same order of magnitude: 7 vs 10 μ M in 'surf'
and 5 vs 8 μ M in 'dcm' layers for LAP and β GLU, respectively. On the other hand, ratios of
enzymatic properties are also relevant information for the interpretation of the ectoenzymatic
hydrolysis of the substrate in terms of quality and quantity. For instance, using high concentration
525 ranges, the LAP K_m is largely higher than β GLU K_m probably because LAP is not adapted to face
low concentration ranges, in contrast to β GLU (Christian and Karl, 1995). However, when the
fluorogenic substrates have the same range of concentration as the natural substrates used by the
enzyme targeted with the fluorogenic substrate, competition for the active sites could be possible.



This increases the risk of overestimating K_m . We thus assumed that K_m , although lower than in
530 published values, are still potentially overestimated. Another difference in response to the tested
range of concentrations for each substrate was the turnover time (K_m/V_m ratio): the lower the
 K_m/V_m , the better the adaptation is to hydrolyze substrates at low concentrations. This should be
considered carefully when comparing reported values.

4.2 Trends with depth

535 We have shown that, depending on the range of concentrations tested, different conclusions can be
drawn regarding the debate about the increase or at least maintenance of specific levels of activity
within deep layers (Koike and Nagata, 1997; Hoppe and Ulrich, 1999; Baltar et al., 2009b). The
trend in vertical depth of activities and cell-specific activities will be discussed below in the context
of the use of different concentration sets for kinetics.

540 In order to compare enzymatic activities between different water masses, from epi- to meso- and
bathypelagic layers, alongside to the decrease with depth of bulk activities, the use of a normalized
activity is required. As most enzymes are produced by heterotrophic prokaryotes, normalization
over total heterotrophic prokaryotic cells is common. However, it is recognized that heterogeneous
545 distribution of single-cell activities among heterotrophic prokaryotes is a recurrent bias in
interpretation of this parameter (Martinez et al., 1996; Hoppe and Ulrich, 1999; Baltar et al.,
2009b). In addition, within epipelagic waters some phytoplankton species also express
ectoenzymatic activity such as AP (Dyhrman and Palenik, 1999, Sebastian and Ammermann 2009,
Lin et al., 2012) and LAP (Martinez and Azam, 1993). At depth, gravitational sinking particles
could retain phytoplankton flocs still showing physiological capacities (Lochte and Turley, 1988;
550 Agusti et al., 2015).

Increasing AP activities per cell with depth has been reported in the Indian Ocean (down to 3000 m-
depth; Hoppe and Ullrich, 1999), in the subtropical Atlantic Ocean (down to 4500 m-depth; Baltar
et al., 2009b) in the central Pacific Ocean (down to 4000 m-depth; Koike and Nagata, 1997). These
authors used high concentrations of MUF-P (250 μM , concentration kinetics from 0.6 to 1200 μM
555 and 150 μM , for these authors, respectively) that could stimulate ectoenzymes of cells attached on
suspended or sinking particles, and thus adapted to face higher concentration ranges. However,
these trends were also obtained using low concentrations (max 5 μM MUF-P), at depths down to
3500 m in the Tyrrhenian Sea (Tamburini et al., 2009). In the bathypelagic layers of the central
Pacific, AP rates accounted for as much as half of that observed in the epipelagic layer but the < 0.2
560 μM dissolved AP was removed to estimate bathypelagic activities (Koike and Nagata, 1997). They
suggested that the deep-sea AP is due to fragmentation and dissolution of rapidly sinking particles.
Indeed, it has been shown that AP determined on concentrated particles had the highest
concentration factor compared to AP of bulk seawater among different tested enzymes (Smith et al.,
1992). Note, however, that our data generally stops in mesopelagic layers (1000 m). Tamburini et
565 al. (2002) obtained a different relative contribution of deep-sea samples when used MUF-P
concentrations were 25 nM or 5 μM at the DYFAMED station in the NW Mediterranean Sea (down
to 2000 m-depth), further showing the artifact of the concentration used. Furthermore, as shown by
these authors, the deep activities could be x1.4 to x2.6 times higher due to the effect of hydrostatic
pressure out of convective periods. With concentration kinetics ending at 50 μM of MUF-P, the
570 specific activities of AP reached using per cell $V_m/50$ or per cell $V_m/1$ were not so different and
their trend with depth were similar (Fig. 8). The particulate matter C/P ratio did not change with



depth whereas DOC/DOP ratio decreased (from 2200-2400 to 1500-1200), suggesting a preference for heterotrophic prokaryotes to use dissolved organic phosphorus as substrate of AP.

For LAP activity, however, Vm50 decreased with depth more intensively than Vm1, but cell-specific LAP showed contradictory results: at all stations cell-specific Vm1 decreased with depth (according to the DVF criterion, Fig. 8) whereas Vm50 remained stable (2 stations over 10) or increased with depth (5 stations over 10). Using a high concentration of MCA-leu other authors have systematically found an increase in LAP activity per cell with depth in bathypelagic layers (Zaccone et al., 2012; Caruso et al., 2013). From our data set, among the two parameters LAP Vm and LAP Km, it is LAP Km which showed the largest differences between the 2 types of kinetics. Km 50 particularly increased with depth more than Km1, and the ratio Km50/Km1 switched from ~16 in epipelagic waters to 121 and 316 in 'liw' and 'mdw' layers, respectively. At many stations (TYR, ION, FAST and ST10), LAP Km1 was stable or decreased with depth whereas LAP Km50 increased, suggesting that within deep layers the LAP activity was more linked to the availability of suspended particles or fresh organic matter associated to sinking material, than to DON. Thus, the difference between Km1 and Km50 might reflect a strategy to adapt to a potential spatial and/or temporal patchiness in the distribution of suspended particles. Freshly sinking material is statistically not included in the bulk, because of the small volume of water incubated, but could contribute to the release of free bacteria, small suspended particles and DOM within its associated plume (Azam and Long, 2001; Tamburini et al., 2003; Grossart et al., 2007; Fang et al., 2014). Baltar et al. (2009a) also suggested that hot spots of activity at depth were associated with particles. The fact that the C/N ratio of particulate material increased (from 11-12 to 22-25) but not that much for DOC/DON (13-12 to 14-15 from 'surf' and 'dcm' to 'liw' and 'mdw', respectively) confirms a preferential utilization of proteins substrates from particles. Recently, Zhao et al. (2020), based on the increasing contribution of genes encoding secretory enzymes, suggested that deep-sea prokaryotes and their metabolism are likely associated with particles rather than on the utilization of ambient-water DOC.

Variation in the relative activities of different enzymes is suggested as a possible indicator of changes of bacterioplankton nutrition patterns along the water column. The LAP/ β GLU ratio decrease with depth follows the decrease of protein to carbohydrate ratio of particulate material (Misic et al., 2002), nitrogen being remineralized faster than carbon. However, here, the TCHO-C/TAA-C ratio was consistently higher within the 'dcm' layer (~90 m) than at the surface and the LAP/ β GLU ratio generally increased also as a consequence. Below the 'dcm' layer, we estimated Vm50 LAP/ β GLU ratios from few of the single rates measured at high concentration (above LOD), and observed an increase with depth. Despite the particulate C/N ratio increasing with depth and TCHO-C/TAA-C increasing in the 'mdw' layer, LAP increased faster than β GLU with depth. Others have also shown an increase of LAP/ β GLU ratio with depth (Hoppe and Ullrich, 1999 in Indian Ocean, Placenti et al., 2018 in the Ionian Sea). Many factors, such as the freshness of the suspended particles, a recent event of convection, a lateral advection from margins, as well as the seasonality and taxonomic composition of phytoplankton could influence dynamics at depth, particularly in the mesopelagic layer (Severin et al. 2016, Caruso et al 2013).

4.3 Regional variability

In epipelagic waters, both AP maximum rates (Vm1, Vm50) significantly increased from the Algerian/Ligurian Basins to the Tyrrhenian Basin (t test, $p = 0.002$ and $p = 0.02$, respectively), and reached maximum values at ION. This longitudinal increase in AP activity was also confirmed by



calculating specific activities which also increased towards ION. This increase of cell-specific AP appears to follow a decrease in DIP availability. While DIP can be assimilated directly through a high affinity absorption pathway, the assimilation of DOP requires that the molecule is first remineralized to separate the DIP from the carbon fraction, using AP enzymes. POP is an indicator of living biomass and enzyme producers, but the correlation between VmAP and POP were negative in the surface layers (log-log relationship, $r = -0.86, -0.88$ for Vm50 and Vm1, respectively), suggesting that POP reflected more the progressive eastward decline of living biomass and its increased capacity to derepress AP genes. VmAP rates in the surface did not correlate with DIP, however the relative DIP deficiency increased eastward, suggested by the deepening of the phosphocline (Table 1), the decrease of average DIP concentration within the phosphate-depleted layer and the decrease in P diffusive fluxes reaching the surface layer (Pulido-Villena et al. 2020, in prep, this issue). Along a trans-Mediterranean transect, Zaccone et al. (2012), did not get any trend between DIP and AP as well, although they found also increased values of AP specific activities in the Eastern Mediterranean Sea. Bogé et al. (2012), using a concentration set close to ours (0.03-30 μM MUF-P) obtained differences in Vm for the 2 types of kinetics (contrary to our results) and described different relationships with DOP and DIP according to the low and high affinity systems. Such differences could be due to the large gradient of trophic conditions in their study, involving a eutrophic bay where DOP and DIP concentration ranged from 0 to 185 nM, and from 0 to 329 nM, respectively. In order to circumvent the effect of depth, correlations are described in our study only for 10 surface data where DIP concentration range is narrow (4-17 nM).

The AP/LAP ratio can be used as an indicator of N - P imbalance as demonstrated in enrichment experiments (Sala et al. 2001). In this study, large concentrations of substrates were used (200 μM) and they described a decrease of the AP/LAP ratio after DIP addition and conversely, a large increase of it (10 fold) after addition of 1 μM nitrate. In their initial experimental conditions, the ratio ranged from 0.2 to 1.9. We observed a similar low ratio in the western Mediterranean Sea, but in the Ionian Sea the AP/LAP reached 17 (Vm50) and 43 (Vm1) suggesting that nutrient stress and imbalance can be as important and variable in different regions of the Mediterranean Sea as observed after manipulation of nutrients.

LAP/ β GLU ratio is used as an index of the ability of marine bacteria to preferentially metabolize proteins rather than polysaccharides. The prevalence of LAP over β GLU is a recurrent observation in temperate areas (Christian and Karl, 1995; Rath et al., 1993) and in high latitudes (Misic et al., 2002, Piontek et al., 2014). For example, LAP/ β GLU ratio varied widely from the Equator to the Southern Ocean, with values from 0.28-to 593 (Sinsabaugh and Shah, 2012). In the Ross Sea, this ratio exhibited a relationship with primary production (Misic et al., 2002). In the Caribbean Sea, along an eutrophic to oligotrophic gradient, the LAP/ β GLU ratio increased toward oligotrophy (Rath and Herndl, 1993). In epipelagic zone, during our study, the degree of trophic conditions exhibited a small gradient of productivity (18 to 35 mg Chla m^{-2}) along the western to the eastern Mediterranean Sea. Following this gradient, LAP/ β GLU ratio ranged from 3 to 17 for Vm50, and from 8 to 34 for Vm1 and thus varied according to the concentration range tested. However we found no statistical significant difference between Tyrrhenian Sea and the western area, due to a high intra-regional variability. Unanue et al. (1999) established biphasic kinetics and obtained a ratio VmLAP / Vm β GLU around 20 for their low concentration range and around 10 for their high concentration range, confirming our results. Finally, the LAP/ β GLU ratios reported in this study and other works using low substrates ranges are still lower than when using higher concentrations: 20-200 in the subarctic Pacific (Fukuda et al., 1995, using 200 μM concentration), 213 at station



ALPHA in the equatorial Pacific (Christian and Karl, 1995, using LLBN instead of MCA-leu at 1000 μM and MUF- βGLU at 1.6 μM), suggesting that the ratio LAP/ βGLU highly changes according to the fluorogenic substrate concentration and not in a regular way.

665 Within deeper layers, cell-specific LAP and cell-specific AP tended to be higher within Tyrrhenian
Sea and ION stations than on the westernmost stations, although comparisons between both areas
were insignificant due to the high intra-regional variability. Azzaro et al. (2012) showed high
seasonal variability in heterotrophic metabolism in the Southern Adriatic Pit, down to 1200 m
depth, and they relied this variability to deep convection events. Tamburini et al. (2002, 2009)
670 noticed also a seasonal variability on deep samples depending on seasonal variability of surface
productivity and particle fluxes. During an intense water column mixing (0-1500 m) in the NW
Mediterranean Sea, Severin et al. (2016) showed that deep-sea convection enhanced bacterial
abundance and bacterial heterotrophic production at depth, resulting in a drastic decline of cell-
specific extracellular enzymatic activities (up to 67%).

4.4 Potential contribution of macromolecules hydrolysis to bacterial production

675 Computation of *in situ* hydrolysis rates demonstrated the direct influence of the determination of
Km and Vm using an appropriate set of fluorogenic concentration to compute rates. TAA
concentrations were lower than Km1 and Km50. The two Michaelis–Menten plots cross each other,
at a substrate value of about $1.8 \pm 1.3 \mu\text{M}$ with LAP and $1.7 \pm 0.6 \mu\text{M}$ with βGLU . Considering the
TAA range, the high affinity system (Km1 Vm1) with its low Km and higher turnover rates gave
680 consequently better *in situ* rates than the low affinity system (Km50 Vm50). Although TCHO
ranges were lower than Km1 but higher than Km50, TCHO was always lower than the crossing
concentration point of the two types of kinetics, and consequently, again, the high affinity system
gave higher *in situ* hydrolysis rates than the low affinity system. If the experimentally added
substrate concentration is clearly above the possible range of concentrations found in the natural
685 environment, *in situ* rates could be largely overestimated. To obtain a significant determination of
the *in situ* rates, the added substrate concentrations should be close to the range of variation
expected in the studied environment (Tamburini et al., 2002).

We compared the *in situ* LAP hydrolysis rates to the N demand of heterotrophic prokaryotes (which
was based on bacterial production data assuming C/N ratio of 5 and no active excretion of
690 nitrogen), and the *in situ* rates of TAA plus TCHO to the bacterial carbon demand (based on a
bacterial growth efficiency of 10% (Gazeau et al, this issue, in prep, C ea et al., 2014, Lem e et al.,
2012). Using the low affinity constants (Vm50 and Km50), hydrolysis of TAA by LAP contributed
only to $25\% \pm 22\%$ of the bacterial N demand in epipelagic layers and $26\% \pm 24\%$ in deep layers.
This contribution increased using the high affinity system ($48\% \pm 29\%$ and $180\% \pm 154\%$ in
695 epipelagic layers and deep layers, respectively). In the North Atlantic, LAP hydrolysis rates of
particles (0.3 μM MCA-leucine added) to bacterial nitrogen demand varied between 63 and 87%,
increasing at 200 m. Crottereau and Delmas (1998) combined kinetics of LAP with combined
amino acid concentrations and found a range of 6 – 121% contribution to bacterial N demand in
aquatic eutrophic ponds. A large variability of LAP hydrolysis to bacterial N demand has been also
700 detected in coastal-estuarine environments using a radiolabeled natural protein as a substrate (2 –
44%, Keil and Kirchman, 1993). Pointek et al. (2014), along a 79°N transect in North Atlantic, used
the turnover of βGLU and LAP determined with 1 μM analog substrate concentrations to compute
in situ TCAA and TCHO hydrolysis rates and showed that 134% and 52% of BP could be
supported by substrates issued from peptide and polysaccharides activities, respectively. Based on a



705 BGE of 10%, these fluxes will represent 10 times less, i.e. 13 and 5% of bacterial carbon demand,
which is in the same order of magnitude as we obtained. In our study, the contribution of TAA
hydrolysis to bacterial N demand is increasing within the ‘dcm’ compared to the ‘surf’ layer (from
means of 10 to 40% based on the high affinity system). This is consistent, however, as some
cyanobacteria can express also LAP (Martinez and Azam, 1993) and *Synechococcus* and
710 *Prochlorococcus* are dominant phytoplankton groups in the Mediterranean Sea (Siokou-Frangou et
al., 2010). In our study, the ‘dcm’ was an active biomass layer where primary production (PP)
peaked (Maranon et al., 2020). Size fractionation of primary production showed the importance of
the phytoplankton excretion, contributing from 20 to 55% to total PP according the stations
(Maranon et al., 2020.). Within the surface mixed layer, other sources of N like atmospheric
715 deposition could sustain a significant part of bacterial N demand. The dry atmospheric deposition
(inorganic+ organic) of N at all the stations within the PEACETIME cruise corresponded to $25 \pm$
17% of bacterial N demand (Van Wambeke et al, in prep).

Likewise, the *in situ* cumulative hydrolysis rates of TCHO by β GLU, estimated only in epipelagic
layers were also ~ 3 times higher using the high affinity system. We summed C sources coming
720 from the hydrolysis by LAP and by β GLU in epipelagic layers (Fig. 10) and compared them to the
bacterial carbon demand. Dissolved proteins and combined carbohydrates contributed only to a
small fraction of the bacterial carbon demand: 1.5% based on the low affinity system constants and
3% based on the high affinity system.

It is only within deeper layers that the hydrolysis rates of TAA were at some stations more
725 important than bacterial N demand, suggesting that proteolysis is one of the major sources of N for
heterotrophic bacteria in aphotic layers. However, it was only based on Vm1 and Km1 kinetic
parameters (i.e. the high affinity system) that we found cases of over-hydrolysis of organic nitrogen
(Fig. 9). This over-hydrolysis was particularly marked in the LIW water mass of the Tyrrhenian
Basin, in which over-hydrolysis up to 220% was obtained as well as higher TAA concentrations in
730 comparison to “older” LIW waters in the Algerian Basin. TAA decreased faster than DON along
LIW trajectory so the labile DON fraction (combined aminoacids) was degraded first. The role of
sedimenting particles or large aggregates associated with attached bacteria are considered as major
providers of labile organic matter for free bacteria (Smith et al., 1992). We could consider that with
the 5 mL volume of water hydrolyzed for TAA analysis, and in the 2 mL water volume used to
735 determine ectoenzymatic kinetics, most of this particulate detrital pool of large size or high density
(i.e. fast sinking particles) is underrepresented, thus the contribution of TAA hydrolysis to bacterial
nitrogen demand is underestimated. However, there is an increasing evidence of secretion not only
of monomers issued from hydrolysis, but also of ectoenzymes produced by particles-attached deep-
sea prokaryotes themselves (Zhao et al., 2020). This could explain why, in a small volume of bulk
740 sea water sample, not representative of large or fast sedimenting particles, we still found biphasic
kinetics. Studying alkaline phosphatase activity in the Toulon Bay, Bogé et al. (2013) observed
biphasic kinetics only in the dissolved phase, which also suggests that AP low affinity system
originates from enzyme secretion from particles. Afterwards, this team focused their research by
size fractionation of particulate material, and they found that the origin of the low affinity system
745 was mostly due to the $> 90 \mu\text{m}$ fraction, i.e. large particles (Bogé et al., 2017).

5 Conclusions

The use of microplate titration technique improved greatly the simultaneous study of different
ectoenzymatic activities. Vertical and regional variability of activities were shown in the



Mediterranean Sea, where heterotrophic prokaryotes face not only carbon, but also N, P limitations.
750 Although biased by the use of artificial fluorogenic substrates, ectoenzymatic activity is an
appropriate tool to study the adaptation of prokaryotes to the large gradients in stoichiometry,
chemical characteristics and quantities of organic matter they face, especially when using a large
panel of concentrations. Further combination of such techniques with the chemical identification of
DOC and DON pools, and meta-omics, as well as the use of marine snow catchers, would help our
755 understanding of the biodegradation of organic matter in a ‘sea of gradients’.

Acknowledgements: This study is a contribution of the PEACETIME project (<http://peacetime-project.org>), a joint initiative of the MERMEX and ChArMEX components supported by CNRS-INSU, IFREMER, CEA, and Météo-France as part of the program MISTRALS coordinated by INSU (doi: 10.17600/17000300). The authors thank also many scientists & engineers for their
760 assistance with sampling/analyses: J Ras for TCHO, R Flerus for TAA, J Guittoneau for nutrients, T Blasco for POC, J Uitz and C Dimier for TChla (analysed at the SAPIGH HPLC analytical service at the IMEV, Villefranche), I Obernosterer, P Catala and B Marie for DOC and bacterial abundances. We warmly thank C Guieu and K Deboeufs, as coordinators of the program PEACETIME.

765

References

- Agusti, S., Gonzalez-Gordillo, J. I., Vaque, D., Estrada, M., Cerezo, M. I., Salazar, G., Gasol, J. M., and Duarte, C. M.: Ubiquitous healthy diatoms in the deep sea confirm deep carbon injection by the biological pump, *Nat. Commun.*, 6, doi: 10.1038/ncomms8608, 2015.
- 770 Aminot, A. and Kérouel, R.: Dosage automatique des nutriments dans les eaux marines, in: *Méthodes d'analyses en milieu marin*, edited by: IFREMER, 188 pp, 2007.
- Arnosti, C.: Microbial Extracellular enzymes and the marine carbon cycle, *Ann. Rev. Mar. Sci.*, 3, 401-425, 2011.
- Arrieta, J. M. and Herndl, G. J.: Assessing the diversity of marine bacterial β -glucosidases by capillary Electrophoresis Zymography, *Appl. Environ. Microb.*, 67, 4896-4900, 2001.
- 775 Azam, F., and Long, R. A.: Sea snow microcosms, *Nature*, 414, 495-498, 2001.
- Azzaro, M., La Ferla, R., Maimone, G., Monticelli, L. S., Zaccone, R., and Civitarese, G.: Prokaryotic dynamics and heterotrophic metabolism in a deep convection site of Eastern Mediterranean Sea (the Southern Adriatic Pit), *Cont.Shelf Res.*, 44, 06-118, doi: 10.1016/j.csr.2011.07.011, 2012.
- 780 Baklouti, M., Diaz, F., Pinazo, C., Faure, V., and Quéguiner, B.: Investigation of mechanistic formulations depicting phytoplankton dynamics for models of marine pelagic ecosystems and description of a new model, *Prog. Oceanogr.*, 71, 1–33, doi :1016/j.pocean.2006.05.002, 2006.
- 785 Baltar, F., Arístegui, J., Gasol, J. M., Sintes, E., and Herndl, G. J.: Evidence of prokaryotic metabolism on suspended particulate organic matter in the dark waters of the subtropical North Atlantic, *Limnol. Oceanogr.*, 54, 182-193, doi:10.4319/lo.2009.54.1.0182, 2009a.
- Baltar, F., Aristegui, J., Sintes, E., van Aken, H. M., Gasol, J. M., and Herndl, G. J.: Prokaryotic extracellular enzymatic activity in relation to biomass production and respiration in the meso- and bathypelagic waters of the (sub)tropical Atlantic, *Env. Microbiol.*, 11, 1998–2014, 2009b.
- 790 Baltar, F.: Watch Out for the “Living Dead”: Cell-Free Enzymes and Their Fate, *Front. Microbiol.*, 8, article 2438, doi: 10.3389/fmicb.2017.02438, 2018.
- Bogé G., Lespilette, M., Jamet, D., and Jamet, J.-L.: Role of sea water DIP and DOP in controlling bulk alkaline phosphatase activity in N.W. Mediterranean Sea (Toulon, France), *Marine Pollution Bulletin*, 64, 1989-1996, doi: 10.1016/j.marpolbul.2012.07.028, 2012.
- 795 Bogé, G., Lespilette, M., Jamet, D. and Jamet, J.-L.: The relationships between particulate and soluble alkaline phosphatase activities and the concentration of phosphorus dissolved in the



- seawater of Toulon Bay (NW Mediterranean). *Mar. Pollut. Bull.*, 74, 413-419, doi: 10.1016/j.marpolbul.2013.06.003, 2013.
- 800 Bogé, G., Lespilette, M., Jamet, D., and Jamet, J.-L.: Role of DOP on the alkaline phosphatase activity of size fractionated plankton in coastal waters in the NW Mediterranean Sea (Toulon Bay, France), *Mar. Pollut. Bull.*, 117, 264-273, doi:10.1016/j.marpolbul.2016.11.037, 2017.
- Caruso, G., Monticelli, L., La Ferla, R., Maimone, G., Azzaro, M., Azzaro, F., Decembrini, F., De Pasquale, F., Leonardi, M., Raffa, F., Zappal, G., and De Domenico, E.: Patterns of
- 805 Prokaryotic Activities and Abundance among the Epi-Meso and Bathypelagic Zones of the Southern-Central Tyrrhenian Sea, *Oceanography*, 1, 1, doi: 10.4172/ocn.1000105, 2013.
- Cauwet, G.: Determination of dissolved organic carbon (DOC) and nitrogen (DON) by high temperature combustion, in: *Methods of Seawater analysis*, edited by: Grashoff, K., Kremling, K. and Ehrhard, M., 3rd Ed., Wiley-VCH, Weinheim, 407-420, 1999.
- 810 Céa, B., Lefèvre, D., Chirurgien, L., Raimbault, P., Garcia, N., Charrière, B., Grégori, G., Ghigliione, J.-F., Barani, A., Lafont, M., and Van Wambeke, F.: An annual survey of bacterial production, respiration and ectoenzyme activity in coastal NW Mediterranean waters: temperature and resource controls, *Environ Sci Pollut Res*, doi: 10.1007/s11356-014-3500-9, 2014.
- 815 Christian, J. R. and Karl, D. M.: Bacterial ectoenzymes in marine waters: Activity ratio and temperature responses in three oceanographic provinces, *Limnol. Oceanogr.*, 40, 1046-1053, 1995.
- Chróst, R.J. *Microbial enzymes in aquatic environments*, Springer-Verlag, New York, 1991.
- Dittmar, T.H., Cherrier, J. and Ludwichowski, K.-U.: The analysis of amino acids in seawater. In:
- 820 *Practical Guidelines for the Analysis of Seawater*, edited by: Wurl, O., Boca Raton, FL: CRC-Press, 67–78, 2009.
- Dyhrman, S. and Palenik, B.: Phosphate stress in cultures and field populations of the dinoflagellate *Prorocentrum minimum* detected by a single-cell alkaline phosphatase assay, *Appl. Environ. Microb.*, 65, 3205-3212, doi: 10.1128/aem.65.7.3205-3212.1999, 1999.
- 825 Engel, A., and Händel, N.: A novel protocol for determining the concentration and composition of sugars in particulate and in high molecular weight dissolved organic matter (HMW-DOM) in seawater. *Mar. Chem.* 127, 180–191, 2011
- Fang, J., Zhang, L., Li, J., Kato, C., Tamburini, C., Zhang, Y., Dang, H., Wang, G., & Wang, F.: The POM-DOM piezophilic microorganism continuum (PDPMC)—The role of piezophilic
- 830 microorganisms in the global ocean carbon cycle, *Science China (Earth Sciences)*, 1–10, doi:10.1007/s11430-014-4985-2, 2014.
- Gazeau, F., Ridame, C., Van Wambeke, F., Alliouane, S., Irisson, J.-O., Marro, S., Grisoni, J.-M., De Liège, G., Nunige, S., Djaoudi, K., Pulido-Villena, E., Dinasquet, J., Obernosterer, I., Catala, P., Guieu, C.: Impact of dust enrichment on Mediterranean plankton communities under
- 835 present and future conditions of pH and temperature: an experimental overview. *Biogeosciences Discuss.*, submitted, this issue.
- Gazeau, F., Van Wambeke, F., Marañón, E., Pérez-Lorenzo, M., Alliouane, S., Stolpe, C., Blasco, T., Zäncker, B., Engel, A., Marie, B., Guieu, C.: Impact of dust enrichment on carbon budget and metabolism of Mediterranean plankton communities under present and future conditions
- 840 of pH and temperature, *Biogeosciences Discuss.*, in prep., this issue.
- Grossart, H.-P., Tang, K. W., Kiørboe, T., and Ploug, H.: Comparison of cell-specific activity between free-living and attached bacteria using isolates and natural assemblages, *FEMS Microb. Lett.*, 266, 194–200, doi:10.1111/j.1574-6968.2006.00520.x, 2007.
- Guieu, C., D'Ortenzio, F., Dulac, F., Taillandier, V., Doglioli, A., Petrenko, A., Barrillon, S.,
- 845 Mallet, M., Nabat, P., and Desboeufs, K.: Process studies at the air-sea interface after atmospheric deposition in the Mediterranean Sea: objectives and strategy of the PEACETIME oceanographic campaign (May–June 2017), *Biogeosciences Discuss.*, <https://doi.org/10.5194/bg-2020-44>, in review, 2020.
- Guyennon, A., Baklouti, M., Diaz, Palmiéri, J., Beuvier, J., Lebeaupin-Brossier, C., Arsouze, T.,
- 850 Beranger, K., Dutay, J.-C., and Moutin, T.: New insights into the organic carbon export in the



- Mediterranean Sea from 3-D modeling, *Biogeosciences*, 12, 25-7046, doi: 10.5194/bg-12-7025-2015, 2015.
- 855 Hoppe, H.-G.: Significance of exoenzymatic activities in the ecology of brackish water: measurements by means of methylumbelliferyl-substrates, *Mar. Ecol. Prog. Ser.*, 11, 299-308, 1983.
- Hoppe, H.-G. and Ullrich, S.: Profiles of ectoenzymes in the Indian Ocean: phenomena of phosphatase activity in the mesopelagic zone, *Aquat. Microb. Ecol.*, 19, 139-148, 1999.
- 860 Hoppe, H.-G., Ducklow, H., and Karrasch, B.: Evidence for dependency of bacterial growth on enzymatic hydrolysis of particulate organic matter in the mesopelagic ocean, *Mar. Ecol. Prog. Ser.*, 93, 277-283, 1993.
- Keil, R.G. and Kirchman, D.: Dissolved combined amino acids: Chemical form and utilization by marine bacteria, *Limnol. Oceanogr.*, 38: 1256-1270, 1993
- Kirchman, D. L.: Leucine incorporation as a measure of biomass production by heterotrophic bacteria. In: *Handbook of methods in aquatic microbial ecology*, edited by: Kemp, P.F., Sherr, B.F., Sherr, E.B. and Cole, J.J., Lewis, Boca Raton, 509-512, 1993.
- 865 Koch, A.L.: Oligotrophs versus copiotrophs, *BioEssays*, 23, 657-661, 2001.
- Koike, I. and Nagata, T.: High potential activity of extracellular alkaline phosphatase in deep waters of the central Pacific, *Deep-Sea Res. PT II*, 44, 2283-2294, 1997.
- 870 Kress, N., Manca, B., Klein, B. and Deponte, D.: Continuing influence of the changed thermohaline circulation in the eastern Mediterranean on the distribution of dissolved oxygen and nutrients: Physical and chemical characterization of the water masses, *J. Geophys. Res. Oceans*, 108, 8109, doi:10.1029/2002JC001397, 2003.
- Krom, M. D., Herut, B. and Mantoura, R. F. C.: Nutrient budget for the eastern Mediterranean: Implication for phosphorus limitation, *Limnol. Oceanogr.*, 49, 1582-1592, doi:10.4319/lo.2004.49.5.1582, 2004.
- 875 Lemée, R., Rochelle-Newall, E., Van Wambeke, F., Pizay, M.-D., Rinaldi, P., and Gattuso, J.-P.: Seasonal variation of bacterial production, respiration and growth efficiency in the open NW Mediterranean Sea., *Aquat. Microb. Ecol.*, 29, 227-237, 2002
- Lindroth, P., and Mopper, K.: High performance liquid chromatographic determination of subpicomole amounts of amino acids by precolumn fluorescence derivatization with o-phthaldialdehyde, *Anal. Chem.* 51, 1667-1674, 1979
- 880 Lin, X., Zhang, H., Cui, Y., and Lin, S.: High sequence variability, diverse subcellular localizations, and ecological implications of alkaline phosphatase in dinoflagellates and other eukaryotic phytoplankton, *Front. Microbiol.*, 3, article 235, doi: 10.3389/fmicb.2012.002352012, 2012.
- 885 Lochte, K. and Turley, C. M.: Bacteria and cyanobacteria associated with phytodetritus in the deep sea, *Nature*, 333, 67-69, 1988.
- Malanotte-Rizzoli P., Manca, B.B., Marullo, S., Ribera d'Alcalà, M., Roether, W., Theocharis, A. and Conversano, F.: The Levantine Intermediate Water Experiment (LIWEX) Group: Levantine basin - A laboratory for multiple water mass formation processes, *J. Geophys. Res.-Oceans*, 108, doi:10.1029/2002JC001643, 2003.
- 890 Marañón, E., Van Wambeke, F., Uitz, J., Boss, E.S., Pérez-Lorenzo, M., Dinasquet, J., Haëntjens, N., Dimier, C., Taillandier, V.: Deep maxima of phytoplankton biomass, primary production and bacterial production in the Mediterranean Sea during late spring, *Biogeosciences Discuss.*, <https://doi.org/10.5194/bg-2020-261>, 2020
- 895 Martinez, J. and Azam, F.: Aminopeptidase activity in marine chroococcoid cyanobacteria. *Appl. Environ. Microb.*, 59, 3701-3707, 1993.
- Martinez, J., Smith, D. C., Steward, G. F., and Azam, F.: Variability in ectohydrolytic enzyme activities of pelagic marine bacteria and its significance for substrate processing in the sea., *Aquat. Microb. Ecol.*, 10, 223-230, 1996.
- 900 Misic, C., Povero, P., and Fabiano, M.: Ectoenzymatic ratios in relation to particulate organic matter distribution (Ross Sea, Antarctica), *Microb. Ecol.*, 44, 224-234, doi:10.1007/s00248-002-2017-9, 2002.



- Piontek, J., Sperling, M., Nothig, E.-V., and Engel, A.: Regulation of bacterioplankton activity in Fram Strait (Arctic Ocean) during early summer: The role of organic matter supply and temperature, *J. Marine Syst.*, 132, 83-94, doi: 10.1016/j.jmarsys.2014.01.003, 2014.
- 905 Placenti, F., Azzaro, M., Artale, V., La Ferla, R., Caruso, G., Santinelli, C., Maimone, G., Monticelli, L. S., Quinci, E. M., and Sprovieri, M.: Biogeochemical patterns and microbial processes in the Eastern Mediterranean Deep Water of Ionian Sea, *Hydrobiologia*, 815, 97-112, doi: 10.1007/s10750-018-3554-7, 2018.
- 910 Pulido-Villena, E., Van Wambeke, F., Desboeufs, K., Petrenko, A., Barrillon, S., Djaoudi, K., Doglioli, A., D'Ortenzio, F., Fu, Y., Gaillard, T., Guasco, S., Nunige, S., Raimbault, P., Taillandier, V., Triquet, S., Guieu, C.: Analysis of external and internal sources contributing to phosphate supply to the upper waters of the Mediterranean Sea (Peacetime cruise), in prep for *Biogeosciences*, special issue PEACETIME.
- 915 Raimbault, P., Pouvesle W., Diaz F., Garcia N., Sempere, R.: Wet-oxidation and automated colorimetry for simultaneous determination of organic carbon, nitrogen and phosphorus dissolved in seawater, *Marine Chemistry* 66, 161-169, 1999.
- Rath, J., and Herndl, G. J.: Characteristics and Diversity of β -D-Glucosidase (EC 3.2.1.21) Activity in Marine Snow, *Appl. Environ. Microbiol.*, 60, 807-813, 1994.
- 920 Sala, M. M., Karner, M., Arin, L., and Marrassé, C.: Measurement of ectoenzyme activities as an indication of inorganic nutrient imbalance in microbial communities, *Aquat. Microb. Ecol.*, 23, 301-311, doi:10.3354/ame023301, 2001.
- Sebastian, M. and Ammerman, J. W.: The alkaline phosphatase PhoX is more widely distributed in marine bacteria than the classical PhoA, *The ISME journal*, 3, 563-572, doi: 10.1038/ismej.2009.102009, 2009.
- 925 Severin, T., Sauret, C., Boutrif, M., Duhaut, T., Kessouri, F., Oriol, L., Caparros, J., Pujo-Pay, M., Durrieu de Madron, X., Garel, M., Tamburini, C., Conan, P., and Ghiglione, J. F.: Impact of an intense water column mixing (0–1500 m) on prokaryotic diversity and activities during an open-ocean convection event in the NW Mediterranean Sea, *Environ. Microbiol.*, 18, 4378-4390, doi:10.1111/1462-2920.13324, 2016.
- 930 Stocker, R.: Marine Microbes See a Sea of gradients, *Science*, 38, 628-633, 2012.
- Sharp, J. H.: Improved analysis for "particulate" organic carbon and nitrogen from seawater, *Limnol.Oceanogr.*, 19, 984-989, 1974.
- Sinsabaugh, R. and Follstad Shah, J.: Ectoenzymatic Stoichiometry and Ecological Theory, *Annu. Rev. Ecol., Evol. S.*, 43, 313-343, doi:10.1146/annurev-ecolsys-071112-124414, 2012.
- 935 Smith, D. C. and Azam, F.: A simple, economical method for measuring bacterial protein synthesis rates in sea water using 3H-Leucine, *Mar. Microb. Food Webs*, 6, 107-114, 1992.
- Smith, D. C., Simon, M., Alldredge, A. L., and Azam, F.: Intense hydrolytic activity on marine aggregates and implications for rapid particle dissolution, *Nature*, 359, 139-142, 1992.
- 940 Taillandier, V., Prieur, L., D'Ortenzio, F., Riberad'Alcala, M., Pulido-Villena, E.: Profiling float observation of thermohaline staircases in the westernMediterranean Sea and impact on nutrient fluxes, *Biogeosciences*, 17, 3343–3366, <https://doi.org/10.5194/bg-17-3343-2020>, 2020
- Tamburini, C., Garcin, J., Ragot, M., and Bianchi, A.: Biopolymer hydrolysis and bacterial production under ambient hydrostatic pressure through a 2000 m water column in the NW Mediterranean. *Deep-Sea Res. PT II*, 49, 2109–2123, doi:10.1016/S0967-0645(02)00030-9, 2002.
- 945 Tamburini, C., Garcin, J., and Bianchi, A.: Role of deep-sea bacteria in organic matter mineralization and adaptation to hydrostatic pressure conditions in the NW Mediterranean Sea, *Aquat. Microb. Ecol.*, 32, 209–218, doi: 10.3354/ame032209, 2003.
- 950 Tamburini, C., Garel, M., Al Ali, B., Mérigot, B., Kriwy, P., Charrière, B., and Budillon, G.: Distribution and activity of Bacteria and Archaea in the different water masses of the Tyrrhenian Sea, *Deep Sea Res.PT II*, 56, 700-714, doi: 10.1016/j.dsr2.2008.07.021, 2009.
- Thingstad, T. F. and Rassoulzadegan, F.: Nutrient limitations, microbial food webs, and 'biological C-pumps': suggested interactions in a P-limited Mediterranean, *Mar. Ecol. Prog. Ser.*, 117, 299-306, 1995.
- 955



- Tholosan, O., Lamy, F., Garcin, J., Polychronaki, T., and Bianchi, A.: Biphase extracellular proteolytic enzyme activity in benthic water and sediment in the North Western Mediterranean Sea, *Appl. Environ. Microb.*, 65, 1619-1626, 1999.
- 960 Unanue, M., Azua, I., Arrieta, J. M., Labirua-Iturburu, A., Egea, L., and Iriberry, J.: Bacterial colonization and ectoenzymatic activity in phytoplankton-derived model particles: Cleavage of peptides and uptake of amino acids, *Microb. Ecol.*, 35, 136-146, doi: 10.1007/s002489900068, 1998.
- 965 Unanue, M., Ayo, B., Agis, M., Slezak, D., Herndl, G. J., and Iriberry, J.: Ectoenzymatic activity and uptake of monomers in marine bacterioplankton described by a biphasic kinetic model, *Microb. Ecol.*, 37, 36-48, doi:10.1007/s002489900128, 1999.
- Van Wambeke, F., Christaki, U., Giannakourou, A., Moutin, T. and Souvemerzoglou, K.: Longitudinal and vertical trends of bacterial limitation by phosphorus and carbon in the Mediterranean Sea. *Microb. Ecol.*, 43, 119-133, doi: 10.1007/s00248-001-0038-4, 2002.
- 970 Van Wambeke, F., Taillandier, V., Deboeufs, K., Pulido-Villena, E., Dinasquet, J., Engel, A., Maranon, E., Guieu, C. : The mixed layer in Mediterranean Sea under the influence of atmospheric deposition: biogeochemical cycles & nitrogen budget after dry & wet deposition events. In prep for Biogeosciences
- Zaccone, R., and Caruso, G.: Microbial enzymes in the Mediterranean Sea: relationship with climate changes, *AIMS Microbiology*, 5, 251-272, 2019.
- 975 Zaccone, R., Caruso, G., Azzaro, M., Azzaro, F., Crisafi, E., Decembrini, F., De Domenico, E., De Domenico, M., La Ferla, R., Leonardi, M., Lo Giudice, A., Maimone, G., Mancuso, M., Michaud, L., Monticelli, L. S., Raffa, F., Ruggeri, G., and Bruni, V.: Prokaryotic activities and abundance in pelagic areas of the Ionian Sea, *Chem. Ecol.*, 26, 169-197, doi: 10.1080/02757541003772914, 2010.
- 980 Zaccone, R., Boldrin, A., Caruso, G., La Ferla, R., Maimone, G., Santinelli, C., and Turchetto, M.: Enzymatic Activities and Prokaryotic Abundance in Relation to Organic Matter along a West-East Mediterranean Transect (TRANSMED Cruise), *Microb. Ecol.*, 64, 54-66, 2012.
- Zhang, J.-Z. and Chi, J.: Automated analysis of nano-molar concentrations of phosphate in natural waters with liquid waveguide, *Environ. Sci. Technol.*, 36, 1048-1053, doi:10.1021/es011094v, 2002.
- 985 Zhao, Z., Baltar, B., and Herndl, G. J.: Linking extracellular enzymes to phylogeny indicates a predominantly particle-associated lifestyle of deep-sea prokaryotes, *Sciences Advances*, 6, eaaz4354, <https://doi.org/10.1126/sciadv.aaz4354>, 2020.



990 Figure Legends

Figure 1. Sampling sites. Color codes on dots correspond to the plots on Fig. 2.

Figure 2. Physical properties along the different sites: a) Oxygen versus depths, b) T/S diagram.

995 Color codes correspond to the stations mapped Fig. 1. Principal water masses are indicated. MAW: Modified Atlantic Waters, LIW: Levantine intermediate Waters, WMDW: Western Mediterranean Deep waters, EMDW: Eastern Mediterranean Deep Waters.

Figure 3. Example of Michaelis-Menten plots, dcm layer at station FAST. Dots are data, continuous
1000 lines the nonlinear regression plot derived from all concentrations added (0.025 to 50 μM). Smallest graphs inside show dotted lines corresponding to regression plots derived from a restricted substrate range (0.025-1 μM).

Figure 4. Distribution of leucine aminopeptidase (LAP) kinetic parameters V_m (a) and K_m (b). Red
1005 values are V_{m50} and K_{m50} derived from the whole substrate MCA-leu range (0.025-50 μM) and pink values are V_{m1} and K_{m1} derived from a restricted substrate range (0.025-1 μM). The bars are not cumulative but absolute values. The error bars are standard errors derived from the nonlinear regressions. At each station four data are presented, corresponding to, from left to right, 'surf', 'dcm', 'liw' and 'mdw' layers, respectively.

1010 Figure 5. Distribution of β glucosidase (βGLU) kinetic parameters V_m (a) and K_m (b). Yellow values are V_{m50} and K_{m50} derived from the whole substrate MCA-leu range (0.025-50 μM) and white values are V_{m1} and K_{m1} derived from a restricted substrate range (0.025-1 μM). The bars are not cumulative but absolute values. The error bars are standard errors derived from the nonlinear
1015 regressions. At each station four data are presented, corresponding to, from left to right, surface and dcm layers, respectively. For 'liw' and 'mdw' layers (black bars) we presented only a mean available rate detectable (kinetics were impossible to compute due to the low range of rates measurable). This value is assumed to represent a minimal value for V_{m50} .

1020 Figure 6. Distribution of alkaline phosphatase (AP) kinetic parameters V_m (a) and K_m (b). Blue values are V_{m50} and K_{m50} derived from the whole substrate MUF-P range (0.025-50 μM) and pale blue values are V_{m1} and K_{m1} derived from a restricted substrate range (0.025-1 μM). The bars are not cumulative but absolute values. The error bars are standard errors derived from the nonlinear regressions. At each station four data are presented, corresponding to, from left to right,
1025 'surf', 'dcm', 'liw' and 'mdw' layers, respectively. V_{m1} and K_{m1} are not available at station FAST mdw layer, due to a lack of significant rates below 1 μM MUF-P added.

Figure 7. Box plot distributions of specific V_{m1} and V_{m50} per bacterial cell, for alkaline
1030 phosphatase (a: per cell $V_{m50\text{AP}}$, b: per cell $V_{m1\text{AP}}$) and leucine aminopeptidase (c: per cell $V_{m50\text{LAP}}$, d: per cell $V_{m1\text{LAP}}$). Box limits 25% and 75% percentiles, horizontal bar is median, red cross is mean, blue dots are outliers.

Figure 8. Depth decreasing factor (DVF, unitless) among different specific activities. DVF is
1035 calculated as the mean of pooled data from 'surf' and 'dcm' layers divided by the mean of pooled data from 'liw' and 'mdw' layers. In red per cell $V_{m50\text{LAP}}$ and per cell $V_{m1\text{LAP}}$: DVF of specific aminopeptidase activities calculated for large (0.025-50 μM) and low (0.025-1 μM) substrate range, respectively; in blue same thing for alkaline phosphatase (per cell $V_{m50\text{AP}}$, per cell $V_{m1\text{AP}}$). For β -glucosidase, specific activities are based on the few detectable rates at high concentration (per cell $V_{\beta\text{glu}}$, yellow dots). Black crosses are specific heterotrophic prokaryotic production per cell
1040 (per cell BP).



Figure 9. In situ hydrolysis rates of dissolved proteins and particulate detrital N-proteins ($\text{nmol N L}^{-1} \text{h}^{-1}$), determined from LAP ectoenzyme kinetics V_{m1}/K_{m1} versus V_{m50}/K_{m50} , and comparison to heterotrophic bacterial nitrogen demand. a) epipelagic layers (surf, dcm), b) deeper layers (liw, mdw)

1045

Figure 10. In situ rates of hydrolysis of dissolved and particulate detrital carbohydrates and C-proteins ($\text{nmol C L}^{-1} \text{h}^{-1}$), determined from LAP and β GLU ectoenzymatic parameters V_{m1} & K_{m1} versus V_{m50} & K_{m50} , and comparison to heterotrophic bacterial carbon demand (BCD) in epipelagic waters. Note the x10 scale for bacterial carbon demand on the right.

1050



Table 1: Characteristics of the stations.

	sampling date	Latitude °N	Longitude °E	bottomdepth m	temp at 5 m °C	depth of 50 nM NO ₃ m	depth of 50 nM DIP m	Integrated Chl a mg chla m ⁻²	depth of '1lw' 'm'lw' water sampled m	depth of water sampled m
ST 10	6/8/2017	37.45	1.57	2770	21.6	30	69	28.9	500	1000
FAST	6/3/2017	37.95	2.92	2775	21.0	50	59	27.3	350	2500
ST 1	5/12/2017	41.89	6.33	1580	15.7	48	76	35.0	500	1000
ST 2	5/13/2017	40.51	6.73	2830	17.0	40	70	32.7	500	1000
ST 3	5/14/2017	39.13	7.68	1404	14.3	47	100	23.2	450	1000
ST 4	5/15/2017	37.98	7.98	2770	19.0	42	63	29.2	500	1000
ST 5	5/16/2017	38.95	11.02	2366	19.5	42	78	30.5	200	1000
TYR	5/17/2017	39.34	12.59	3395	19.6	82	95	31.3	200	1000
ST 6	5/22/2017	38.81	14.50	2275	20.0	43	113	18.7	400	1000
ION	5/25/2017	35.49	19.78	3054	20.6	85	231	27.7	250	3000



Table 2. Microbial abundances and fluxes at the 4 layers studied for ectoenzymatic activities. Means \pm sd and range values given for all stations (n=10), and both range of concentrations tested (up to 50 or up to 1 μ M). Maximum velocity rates (Vm50 and Vm1), half saturation constants (Km50 and Km1) for leucine aminopeptidase (LAP), β -glucosidase (β GLU), alkaline phosphatase (AP), bacterial abundance (BA) and heterotrophic prokaryotic production (BP). ld limits of detection, not enough data to plot Michaelis-Menten kinetics

		surface	dcm	liwlayers	mdw waters
Vm50 LAP nmol l ⁻¹ h ⁻¹	mean \pm sd	1.00 \pm 0.78	1.20 \pm 0.92	0.26 \pm 0.24	0.17 \pm 0.13
	range	0.36 – 2.85	0.33 – 2.83	0.08 – 0.91	0.06 – 0.45
Vm1 LAP nmol l ⁻¹ h ⁻¹	mean \pm sd	0.29 \pm 0.10	0.45 \pm 0.25	0.028 \pm 0.014	0.017 \pm 0.010
	range	0.21 – 0.56	0.19 – 0.98	0.014 – 0.060	0.007 – 0.042
Vm50 β GLU nmol l ⁻¹ h ⁻¹	mean \pm sd	0.13 \pm 0.04	0.12 \pm 0.08	ld	ld
	range	0.08 – 0.23	0.03 – 0.30		
Vm1 β GLU nmol l ⁻¹ h ⁻¹	mean \pm sd	0.019 \pm 0.009	0.025 \pm 0.019	ld	ld
	range	0.012 – 0.040	0.014 – 0.077		
Vm50 AP nmol l ⁻¹ h ⁻¹	mean \pm sd	2.56 \pm 2.58	3.73 \pm 4.52	0.38 \pm 0.48	0.25 \pm 0.40
	range	0.30 – 8.30	0.11 – 14.6	0.04 – 1.66	0.06 – 1.30
Vm1 AP nmol l ⁻¹ h ⁻¹	mean \pm sd	1.55 \pm 1.58	3.01 \pm 4.01	0.02 \pm 1.11	0.12 \pm 0.25
	range	0.25 – 5.62	0.07 – 13.2	0.24 – 0.33	0.01 – 0.80
Km50 LAP μ M	mean \pm sd	7.4 \pm 6.9	5.2 \pm 7.7	17.8 \pm 15.2	22.3 \pm 26.3
	range	0.8 – 20.9	0.4 – 25.0	3.6 – 41.6	1.8 – 83.8
Km1 LAP μ M	mean \pm sd	0.50 \pm 0.20	0.42 \pm 0.28	0.23 \pm 0.19	0.25 \pm 0.27
	range	0.12 – 0.83	0.07 – 0.90	0.10 – 0.69	0.01 – 0.88
Km50 β GLU μ M	mean \pm sd	10.6 \pm 6.3	8.7 \pm 7.2	ld	ld
	range	4.4 – 27.4	1.2 – 24.3		
Km1 β GLU μ M	mean \pm sd	0.044 \pm 0.071	0.11 \pm 0.11	ld	ld
	range	0.009 – 0.244	0.01 – 0.36		
Km50 AP μ M	mean \pm sd	0.72 \pm 0.71	0.49 \pm 0.34	2.25 \pm 2.42	3.7 \pm 6.8
	range	0.09 – 2.18	0.18 – 1.07	0.17 – 7.32	0.4 – 21.9
Km1 AP μ M	mean \pm sd	0.11 \pm 0.03	0.27 \pm 0.28	0.37 \pm 0.22	0.27 \pm 0.16
	range	0.07 – 0.14	0.05 – 0.80	0.14 – 0.89	0.06 – 0.52
BA 10 ⁵ cells ml ⁻¹	mean \pm sd	5.3 \pm 1.6	5.4 \pm 1.5	1.13 \pm 0.40	0.56 \pm 0.15
	range	2.1 – 7.8	4.0 – 8.5	0.41 – 1.91	0.33 – 0.78
BP ng C l ⁻¹ h ⁻¹	mean \pm sd	37 \pm 13	21 \pm 7	0.77 \pm 0.40	0.27 \pm 0.19
	range	26 – 64	12 – 32	0.39 – 1.60	0.07 – 0.60



Table 3 Range of different potential specific activities calculated using Vm derived from the low range of concentration tested (25 to 1000 nM fluorogenic substrates; Vm1), and specific to either i) abundance of total heterotrophic prokaryotes (per cell activities), ii) heterotrophic bacterial production (per unit BP) and iii) particulate organic matter: nitrogen (PON) for LAP, carbon (POC) for βGLU and phosphorus (POP) for AP. DVFs the ‘depth decreasing factor’, calculated for each station as mean value in epipelagic water (surface and dcm data) divided by the mean in deep waters (low and mdw data). The distribution of cell specific Vm1 and cell specific Vm50 for AP and LAP are also presented on Fig 7.

enzyme	units	surface	dcm	lw	mdw	DVF
Per cell LAP	10 ¹⁸ mol leu bact ⁻¹ h ⁻¹	0.33-1.52	0.44-2.18	0.11-0.70	0.12-0.54	1.3-9.6
Per cellβGLU	10 ¹⁸ mol glucose bact ⁻¹ h ⁻¹	0.02-0.11	0.02-0.17	nd	nd	nd
Per cell AP	10 ¹⁸ mole P bact ⁻¹ h ⁻¹	0.45-26	0.11-32	0.13-11	0.17-23	0.1 - 28
Per cell BP	10 ¹⁸ g C bact ⁻¹ h ⁻¹	46-136	25-60	3-17	1-14	4-23
per BP LAP	nmol AA nmol C ⁻¹	0.04-0.24	0.12-0.44	0.21-1.08	0.36-3.03	0.09-0.76
per BP βGLU	nmol glucose nmol C ⁻¹	0.003-0.017	0.007-0.034	nd	nd	nd
per BP AP	nmol P nmol C ⁻¹	0.09-2.3	0.05-11	0.46-8	0.6-40	0.04-1.7



Table 4. Turnover times of ectoenzymes (Km/Vm ratio). Means \pm sd and range values given for all stations (n = 10). For leucine aminopeptidase (LAP), beta glucosidase (β GLU), alkaline phosphatase (AP). ld limits of detection, not enough data to plot Michaelis Menten kinetics. The turnover times are calculated from concentration kinetics using up to 50 μ M concentration or up to 1 μ M concentration.

Units: days		surface	dcm	liw layers	mdw waters
Km50/Vm50 LAP	mean \pm sd	309 \pm 214	144 \pm 186	2912 \pm 1756	4526 \pm 2118
	range	94-880	40-663	1294-6616	1308-7791
Km1/Vm1 LAP	mean \pm sd	75 \pm 28	41 \pm 22	345 \pm 235	634 \pm 713
	range	15-120	15-82	141-985	55-2481
Km50/Vm50 β GLU	mean \pm sd	3464 \pm 1576	3091 \pm 1551	ld	ld
	range	1997-7395	328-5481	nd	nd
Km1/Vm1 β GLU	mean \pm sd	126 \pm 233	247 \pm 273	ld	ld
	range	20-784	15-873	nd	nd
Km50/Vm50 AP	mean \pm sd	18 \pm 20	39 \pm 46	563 \pm 542	1042 \pm 1156
	range	2-69	0.7 – 113	16 – 1441	20 – 3875
Km1/Vm1 AP	mean \pm sd	5.6 \pm 5.0	27 \pm 37	268 \pm 349	301 \pm 172
	range	1-17	0.6-106	12-1180	14-594



Fig 1

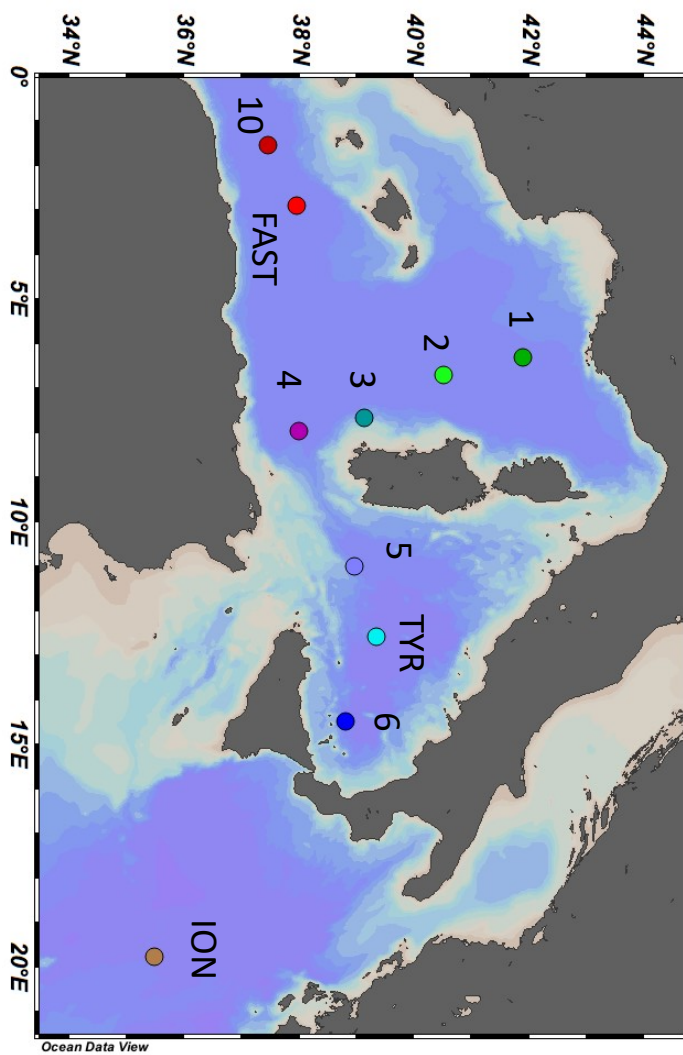




Fig 2

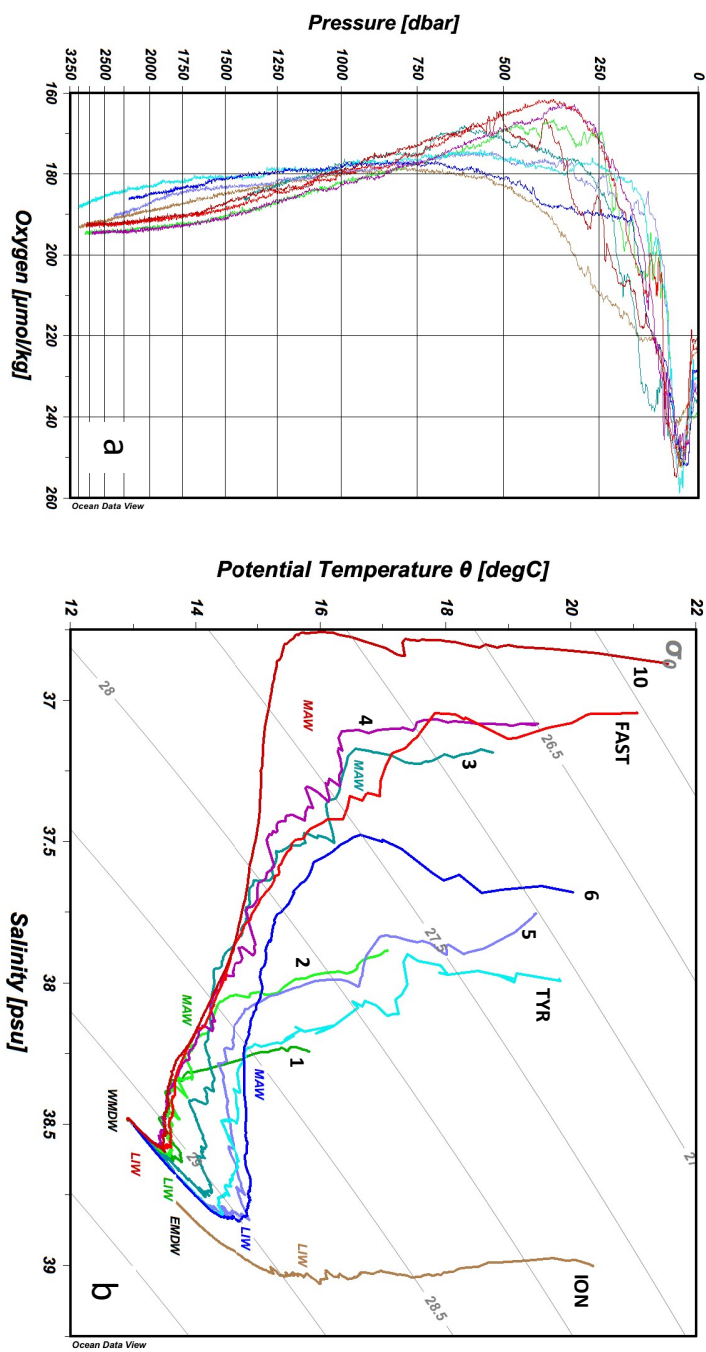




Fig 3

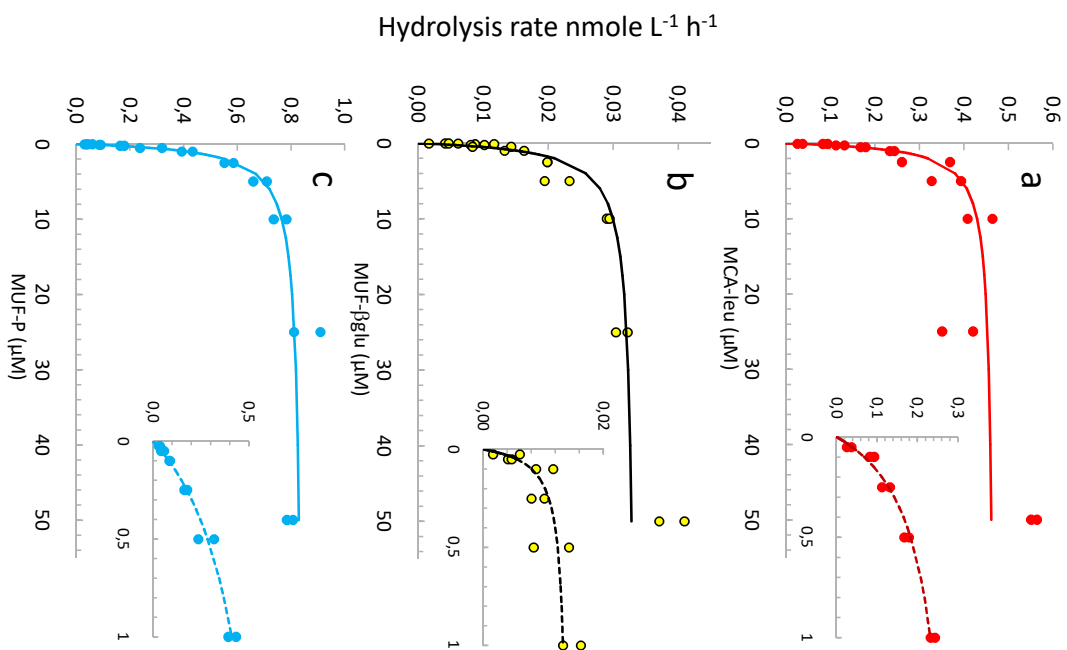




Fig 4

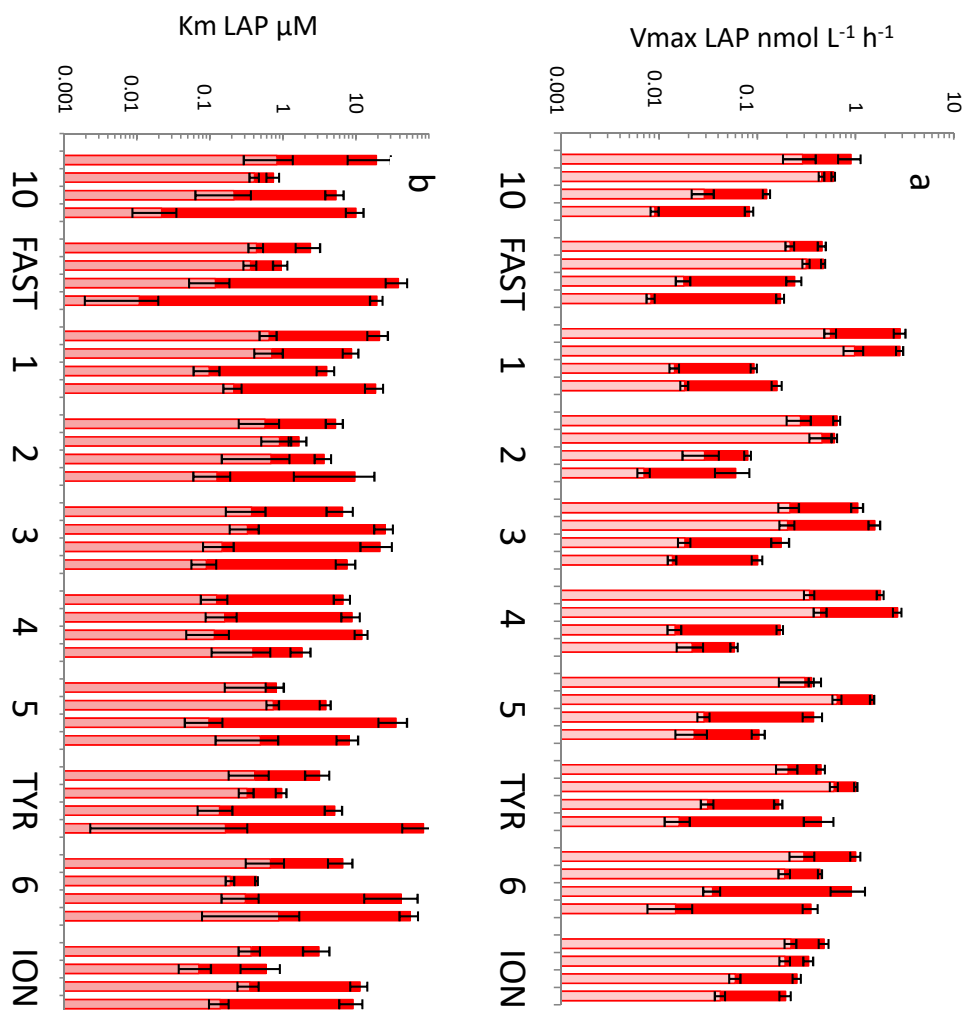
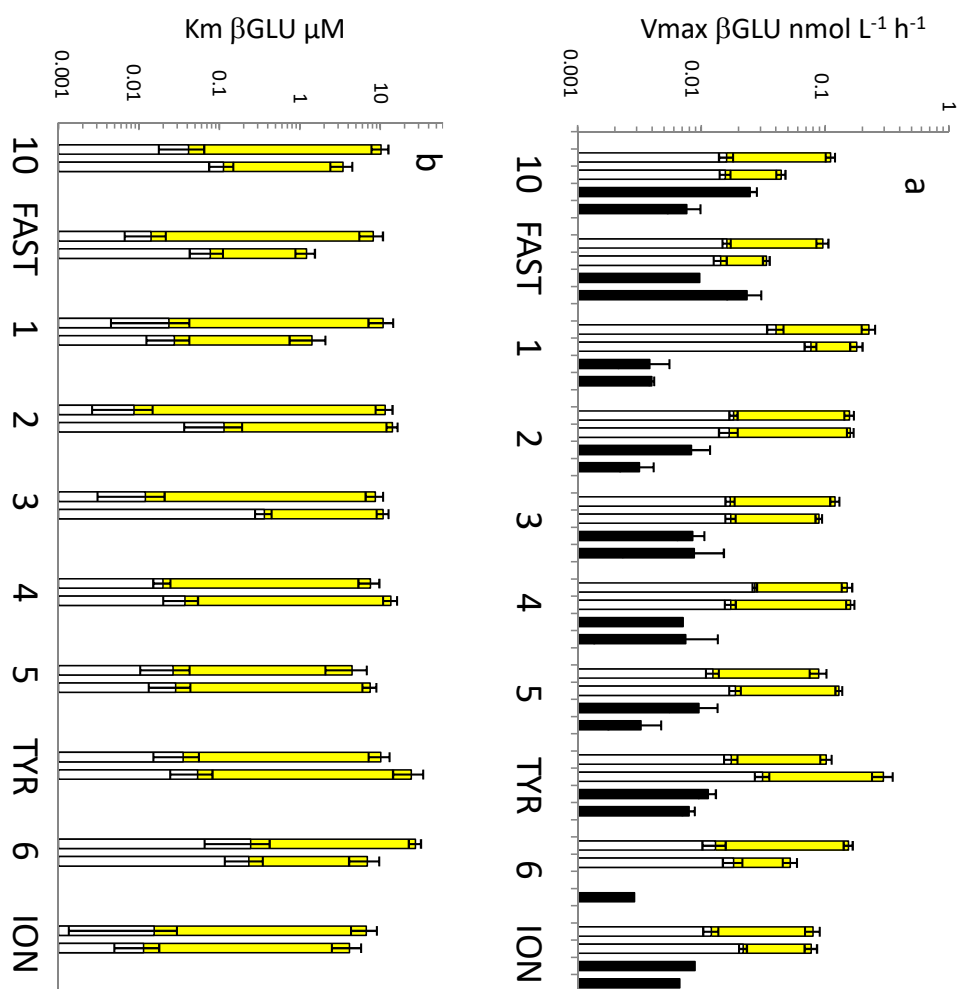




Fig 5



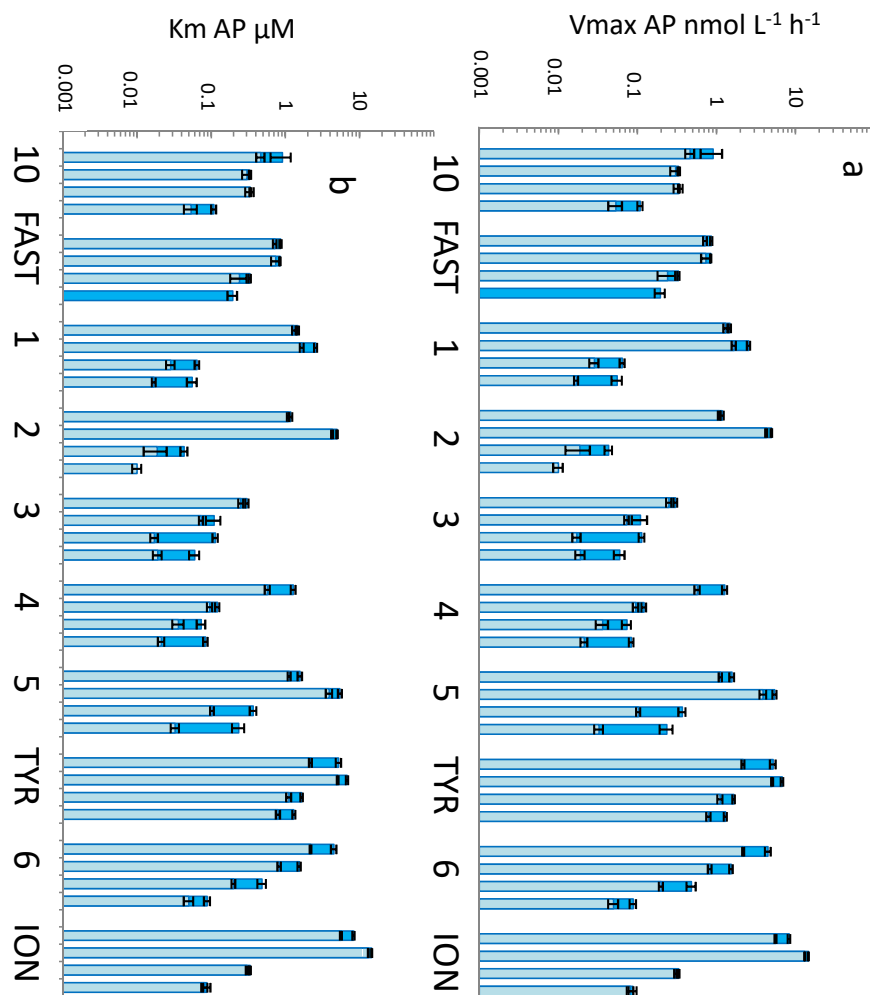




Fig 7

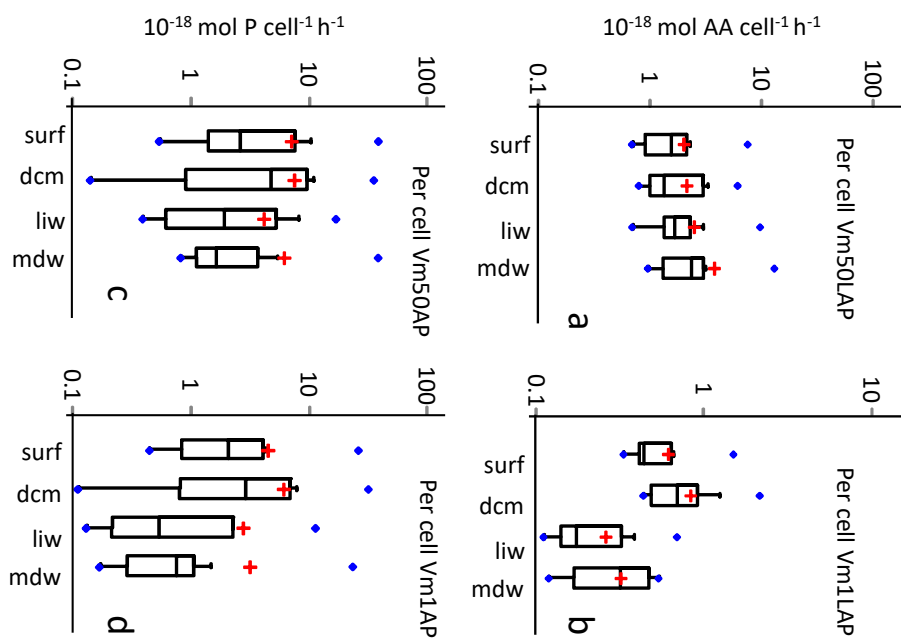




Fig 8

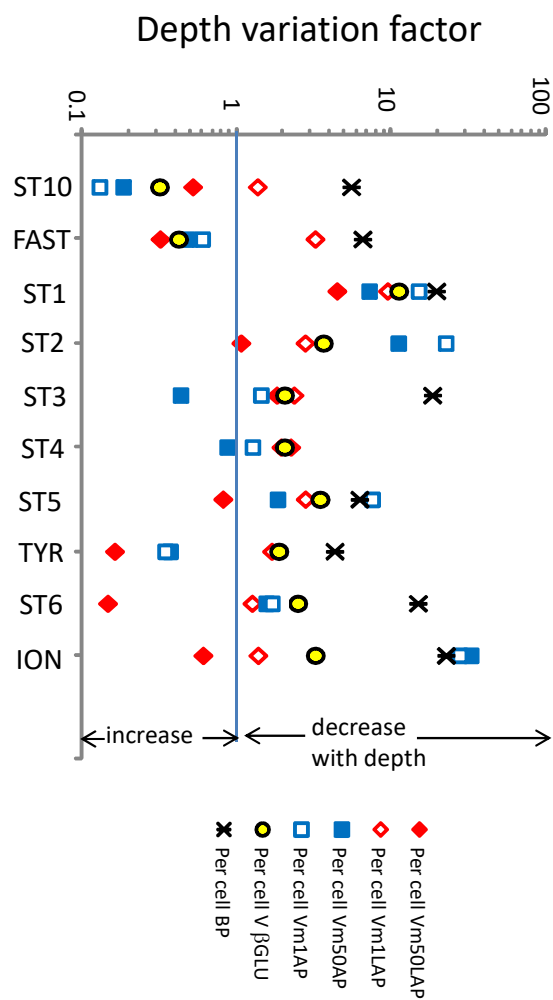




Fig 9

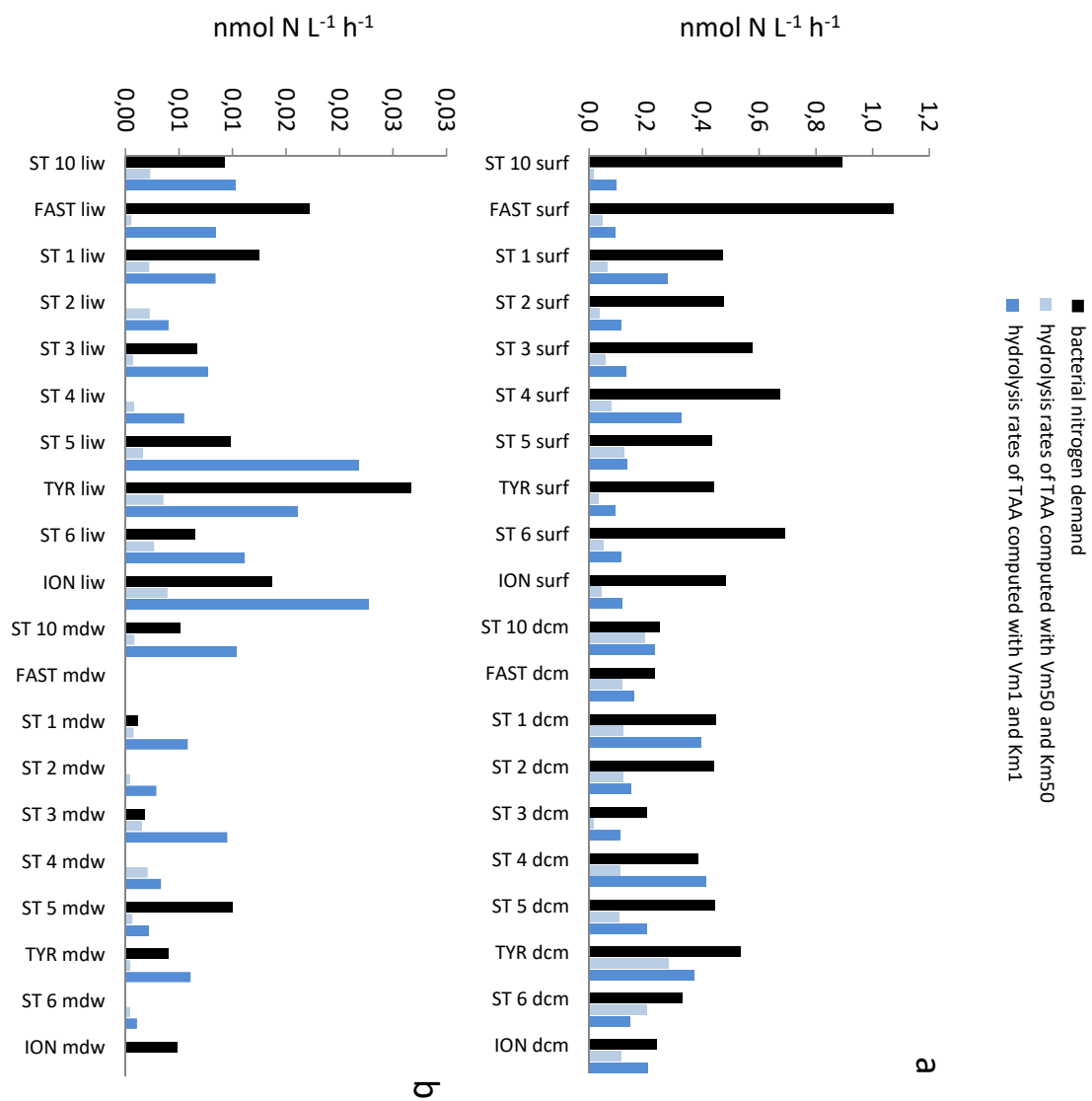




Fig 10

